

Semi-classical generalized Langevin equation for equilibrium and nonequilibrium molecular dynamics simulation

Jing-Tao Lü^a, Bing-Zhong Hu^a, Per Hedegård^b, Mads Brandbyge^c

^a*School of Physics and Wuhan National High Magnetic Field Center, Huazhong University of Science and Technology, 430074 Wuhan, P. R. China*

^b*Niels-Bohr Institute & Nano-science Center, University of Copenhagen, 2100 Copenhagen Ø, Denmark*

^c*Department of Micro- and Nanotechnology, Technical University of Denmark, DK-2800 Kongens Lyngby, Denmark*

Abstract

Molecular dynamics (MD) simulation based on Langevin equation has been widely used in the study of structural, thermal properties of matters in different phases. Normally, the atomic dynamics are described by classical equations of motion and the effect of the environment is taken into account through the fluctuating and frictional forces. Generally, the nuclear quantum effects and their coupling to other degrees of freedom are difficult to include in an efficient way. This could be a serious limitation on its application to the study of dynamical properties of materials made from light elements, in the presence of external driving electrical or thermal fields. One example of such system is single molecular dynamics on metal surface, an important system that has received intense study in surface science. In this review, we summarize recent effort in extending the Langevin MD to include nuclear quantum effect and their coupling to flowing electrical current. We discuss its applications in the study of adsorbate dynamics on metal surface, current-induced dynamics in molecular junctions, and quantum thermal transport between different reservoirs.

Keywords: Semi-classical generalized Langevin equation, molecular dynamics, current-induced dynamics

1. Introduction

The Langevin equation has been widely used to describe the dynamics of open systems interacting with an environment (bath). Their interaction introduces dissipation and fluctuations to the system[1–3], which are incorporated into the Langevin equation as friction and noise terms. When the time scale of the particle is comparable to that of the environmental degrees of freedom (DoF), the frictional force felt by the particle will have a memory kernel, meaning that the friction acting on the particle depends on the velocity at an earlier time. This leads to the generalized Langevin equation (GLE)[4–8]. By solving the GLE, different equilibrium and nonequilibrium mechanical, thermal properties of the system can be extracted.

Although the studied system could be made from different kinds of DoF[9], the most widely studied one is nuclear or atomic or phononic DoF under the influence of thermal baths[10–18]. Interesting applications include the study of nuclear quantum effects[17–26], heat transport between two different thermal baths[12–16, 27–37], scattering of single molecule on surfaces[38–56], and so on.

Classical GLEs derived from Newtonian equation of motion can also be extended to the quantum mechanical regime, using the Heisenberg equation of motion[57], the influence functional approach of Feynman & Vernon[58], and the density matrix method[59, 60]. Caldeira and Leggett successfully used the influence functional approach to study quantum tunneling in macroscopic systems and dynamics of quantum Brownian motion[61, 62]. In these studies, the environment is modeled by an infinite set of harmonic oscillators occupied by the quantum mechanical Bose-Einstein distribution with the zero-point fluctuations included. The bilinear coupling of the system to the quantum reservoir introduces partial quantum mechanical effects to the system, even if the system itself follows the classical equations of motion[61–67]. This semi-classical GLE (SGLE) has been used recently to study the nuclear

Email address: jtl1u@hust.edu.cn (Jing-Tao Lü)

quantum effect [17, 18, 68–70]. If the system couples to reservoirs with different temperatures, it can also be used to study the dynamics of heat transport [12, 14, 29, 33].

The extension of the influence functional approach to consider the electronic reservoir was also conducted by several researchers and compared to harmonic oscillator reservoir[71–74]. It has been used to study muon diffusion in metals, single molecule scattering, vibrational relaxation on metal surface, and so on. The electron-hole pair (EHP) excitation is the origin of the friction force felt by the system, termed electronic friction[75–81]. In surface science, molecular dynamics (MD) incorporating electronic friction has proven useful in the study of adsorbate dynamics on metal surface, where the metal electrons couple to the atomic DoF and damp their motion[81].

In the important new case of a nonequilibrium electron environment, i.e., in the presence of electrical current, the SGLE can also be used to study current-induced forces and Joule heating in molecular conductors and nanomechanical systems[82–99].

The scope of present review is to summarize recent advances and applications of the SGLE to model MD in contact with electronic and phononic reservoirs possibly in nonequilibrium situations. First, we will briefly sketch the derivation of the SGLE from the influence functional approach, taking an electronic reservoir as an example. Within the harmonic approximation, we will analyze the effect of the non-thermal, nonequilibrium electronic environment on the nuclear dynamics. This is followed by several applications in the study of thermal transport, nuclear quantum effects, and current-induced dynamics. Finally, we give a brief summary and perspective for future developments.

2. Theory

Our starting point is the separation of the whole world into system and environment. Here the system is the atomic DoF that we are interested in, and the environment is the rest of the world. Our goal is to derive an equation of motion for the system DoF. The first step is to write down equations of motion for the system plus the environment DoF. We then eliminate the environment degrees of freedom and obtain effective equations of motion of the system including the effects of the environment, yielding dissipation and fluctuation terms.

Different approaches can be used to perform this procedure[6, 8, 10–16, 27–29, 53, 57–62, 71–73, 100–102]. Our choice is the influence functional approach of Feynman and Vernon[58]. In this approach, one starts with the full density matrix including both electrons and nuclei. Selecting the system as the nuclear DoF that one is interested in, one tries to obtain the reduced density matrix of the system only. This is realized by tracing out the environment DoF. The influence functional describes the effect of the environment on the system. From the reduced density matrix, one then performs an expansion over the classical nuclear paths to the second order, taking the deviation from the classical path as perturbation. It has at least two advantages: (1) it can deal with both boson and fermion reservoirs; (2) the reservoirs may be in a nonequilibrium state due to external driving[8]. A system coupling to a bath of harmonic oscillators has been considered in seminal works by Feynman and Vernon[58], Caldeira and Leggett[61, 62]. We here take a noninteracting electronic reservoir as an example.

2.1. Influence functional

We only give a sketch of the derivation and the details can be found in our earlier works[87, 90]. We consider a system including electrons and nuclei. The total Hamiltonian has two parts

$$H = H_e(x) + H_I. \quad (1)$$

The nuclear Hamiltonian takes the standard form, including the kinetic and the potential energy terms

$$H_I = \sum_i \frac{p_i^2}{2M_i} + V_I(x). \quad (2)$$

The electrons couple to the nuclear DoF through a displacement dependent Hamiltonian $H_e(x)$, where x represents a vector made from displacement of the nuclear DoF

$$H_e(x) = \int dr \Psi(r)^\dagger [H_0 + H_{el}(x)] \Psi(r). \quad (3)$$

Here, H_0 is purely electronic, the coupling to nuclear DoF is in $H_{el}(x)$, through its dependence on x . The operators $\Psi(r)$ and $\Psi(r)^\dagger$ are the creation and annihilation field operator of electrons, and r represents the electron position. Here, we did not include the electron-electron interaction explicitly. We assume that H_e represents either a single electron Hamiltonian, or includes electron-electron interaction at a mean field level, like by density functional theory (DFT).

The reduced density matrix of the system in the displacement representation $\rho_s(x, y, t)$ can be written as

$$\rho_s(x_2, y_2, t_2) = \int dx_1 \int dy_1 \mathcal{K}(x_2, y_2, t_2; x_1, y_1, t_1) \rho_s(x_1, y_1, t_1), \quad (4)$$

with the propagator of the reduced density matrix being (we use $\hbar = 1$ in all formulas throughout the paper)

$$\mathcal{K}(x_2, y_2, t_2; x_1, y_1, t_1) = \int_{x_1}^{x_2} \mathcal{D}x \int_{y_1}^{y_2} \mathcal{D}y e^{i[S_s(x) - S_s(y)]} F(x, y). \quad (5)$$

Here, x and y are a pair of displacement histories of the nuclei from time t_1 to time t_2 , (x_1, x_2) and (y_1, y_2) correspond to the forward and backward propagating paths of the reduced density matrix, and $S_s(x)$ and $S_s(y)$ are the system action along these two paths, respectively. The influence functional $F(x, y)$ includes the information of coupling to the electronic environment via the electronic time-propagators on forward and backward paths, $U(t, x)$ and $U(t, y)$, respectively,

$$F(x, y) = \text{Tr}_e[\rho_e U^\dagger(t, y) U(t, x)] / \text{Tr}_e[\rho_e]. \quad (6)$$

Here, ρ_e is the initial density matrix of the electron reservoir when the nuclei are at their initial positions.

At this stage, it is convenient to introduce two new variables, which are the average and difference of the forward x and backward y displacement, respectively

$$R(t) = \frac{1}{2}[x(t) + y(t)], \quad \xi(t) = x(t) - y(t). \quad (7)$$

The average path $R(t)$ describes the propagation of the diagonal matrix element of the reduced nuclear density matrix $\rho_s(R + \xi/2, R - \xi/2)$. Its propagator can be written in terms of the new variables

$$\mathcal{K}(R_2, \xi_2, t_2; R_1, \xi_1, t_1) = \int_{R_1}^{R_2} \mathcal{D}R \int_{\xi_1}^{\xi_2} \mathcal{D}\xi e^{i[S_s(R+\xi/2) - S_s(R-\xi/2)]} F(R + \xi/2, R - \xi/2). \quad (8)$$

The action of the nuclear part is

$$\begin{aligned} S_s(R + \xi/2) - S_s(R - \xi/2) &= \int_{t_1}^{t_2} dt' \left[M\dot{R}\dot{\xi} - V_I(R + \xi/2) + V_I(R - \xi/2) \right] \\ &\approx - \int_{t_1}^{t_2} dt' \left[M\ddot{R} + \frac{\partial V_I(R)}{\partial R} \right] \xi. \end{aligned} \quad (9)$$

Here, $\dot{R} = \partial R / \partial t'$ is derivative with respect to time t' , and we have omitted the time arguments. In the second equation, we have performed an integration-by-part. The boundary terms are ignored when performing the integration-by-part since they merely contribute to a normalization factor to \mathcal{K} . It can be shown that the term quadratic in ξ is zero. Thus, to the second order in ξ , we get the classical nuclear equation of motion if we perform the integral over ξ . This shows that, $R(t)$ is actually the classical path that the nuclei would follow, and ξ measures the fluctuations away from the classical path.

The key problem next is to evaluate $F(x, y)$, and write it as an expansion in ξ . Here, we consider two models of the electron-nuclear interaction. One is the *adiabatic* approximation where the ionic velocity \dot{x} is the small parameter, utilizing the fact that nuclear mass is much larger than that of electrons. In this case we can perform an expansion over \dot{x} (small- \dot{x} expansion). In so doing, we may deal with large displacements or even diffusion of the nuclei. The resulting Langevin equation becomes Markovian due to the time scale separation of electronic and nuclear DoF. The other approach is to take the displacement itself, x , to be small. In this case, the nuclei oscillate in a small region around their equilibrium positions and we can do a perturbation expansion over x (small- x expansion). The timescale of nuclei does not have to be much smaller than that of electrons. Thus, it results in a generalized Langevin equation with memory kernel.

2.2. Adiabatic expansion

Following the standard Fermionic path integral approach, we can write the terms in $F(x, y)$ as functional integral of the electronic Grassmann fields ψ and ψ^* ,

$$F(x, y) = \text{Tr}_e \left[\rho_e U^\dagger(t, y) U(t, x) \right] = \int \mathcal{D}(\psi^* \psi) \quad (10)$$

$$\times \exp \left[i \int_\gamma d\tau \int dr \psi^*(r, \tau) \left(i \frac{\partial}{\partial \tau} - H_e(\tau) \right) \psi(r, \tau) \right].$$

We have combined the forward and backward propagation into one contour with time τ , x and y are then paths on the upper and lower branches of the contour. The electron fields satisfy the boundary condition $\psi(r, t_1) = -\psi(r, t_2)$.

In the adiabatic (small- \dot{x}) approximation, assuming the nuclear dynamics is much slower than that of the electrons in the environment, we can perform an expansion over the Born-Oppenheimer eigenfunctions $\phi_n(\tau)$ corresponding to $H_e(t)$ at time t

$$\psi(x(\tau)) = \sum_n a_n(\tau) \phi_n(x(\tau)). \quad (11)$$

The action of the electrons can be written as

$$S_e = a^*(G_0^{-1} + V)a, \quad (12)$$

with $V_{mn}(\tau, \tau') = i \langle \phi_m(\tau) | \dot{\phi}_n(\tau') \rangle$. We are here employing a very condensed notation, where the time dependence and n dependence of $a_n(\tau)$ is suppressed, and two integrals over times and sums over n are understood, much like the Einstein summation notation, known from relativity theory. The Green's functions G_0 is diagonal in the n variable and the diagonal elements are given by

$$\left(i \frac{\partial}{\partial \tau} - \varepsilon_n(\tau) \right) G_{0mn}(\tau, \tau') = \delta(\tau, \tau'). \quad (13)$$

In this way, the functional integral can be performed formally,

$$\int \mathcal{D}(a^* a) e^{iS_e} = \det(G_0^{-1} + V) = \exp \left[\text{Tr} \ln(G_0^{-1} + V) \right]$$

$$\approx \exp \left[\text{Tr} \ln G_0^{-1} + \text{Tr}(G_0 V) - \frac{1}{2} \text{Tr}(G_0 V G_0 V) \right]. \quad (14)$$

We have expanded it to the 2nd order in the interaction V . Actually, we can rewrite V as,

$$V_{mn}(t', t) = i \langle \phi_m(t') | \dot{\phi}_n(t) \rangle = i \langle \phi_m(t') | \partial_{x_j} \phi_n(t) \rangle \dot{x}_j. \quad (15)$$

After some manipulation of the influence functional, we can show that: (1) The first term in Eq. (14) contributes with an effective Born-Oppenheimer potential (V_e) to the effective action; (2) The second term contributes to a term $\propto \dot{x}(y)$ and linear in ξ ; (3) The third term contributes to a term quadratic in ξ . The total effective action of system can then be written as,

$$S_{\text{tot}} = - \int_{t_1}^{t_2} dt' \int_{t_1}^{t_2} dt'' \left[\xi(t') \left(M \ddot{R}(t') + \frac{\partial V_I(R(t'))}{\partial R} + \frac{\partial V_e(R(t'))}{\partial R} + \Gamma_e \dot{R}(t') \right) \right. \\ \left. + \frac{i}{2} \xi(t') \Pi(t', t'') \xi(t'') \right]. \quad (16)$$

The effect of the electronic environment on the system dynamics can be deduced from the effective action. The nuclear equation of motion gains two extra terms related to the coupling to the environment. The first is the Born-Oppenheimer force, and the second is the electronic friction. Moreover, quantum fluctuations around the classical path $R(t)$ shows up in the term second order in ξ . With the help of the Hubbard-Stratonovich transformation, its effect on the equation of motion can be interpreted as a classical Gaussian noise acting on the system. The final result is

a semi-classical Langevin equation[63], which describes the stochastic classical system within a quantum electronic environment[103–105]

$$\ddot{X} = F_I(X) + F_e(X) - \Gamma_e \dot{X} + \chi_e. \quad (17)$$

Here, X represents a vector made from the mass-renormalized displacements $X = (\cdots, \sqrt{M_i}R_i, \cdots)$, F_I and F_e are the nuclear and the Born-Oppenheimer force, respectively, and Γ_e is the friction matrix. The fluctuating force χ_e describes the quantum and thermal fluctuations away from the classical path $R(t)$ in S_{tot} . Its average is zero, and the correlation function is $\langle \chi(t)\chi(t') \rangle = \Pi(t, t')$, which can also be expressed from G_0 and V [87]. In equilibrium, it is described by the fluctuation-dissipation relation: $\langle \chi(\omega)\chi^*(\omega) \rangle_{\text{eq}} = \omega\Gamma_e \coth(\omega/2k_B T)$. Thus, we have a colored noise with frequency dependence. It reduces to white noise in the high temperature, classical limit, $\langle \chi(\omega)\chi^*(\omega) \rangle_{\text{eq}} = 2\Gamma_e k_B T$.

Similar equations have been derived using the scattering theory approach[93, 93, 106]. The concept of electronic friction Γ_e has been widely used to describe the energy dissipation in the study molecular scattering, diffusion, rotational and vibrational relaxation on metal surfaces under external stimulation. In these studies, it is crucial that the displacement of the nuclei could be very large, and the parameters entering the SGLE may depend on the position of the nuclei. We will discuss this issue in Sec. 4.

2.3. Perturbation expansion

Alternatively, we can perform an expansion over the displacement x . To do that, we consider the linear in x term in $H_{el}(x)$, and assume x is small. This results in a linear electron-phonon coupling term

$$H_{el} \approx \left. \frac{\partial H_{el}}{\partial x} \right|_{x_0} x \equiv M^x x. \quad (18)$$

An expansion over x to the second order results in a SGLE of the following form in mass-scaled displacement,

$$\ddot{X}(t) - F_I(X(t)) = - \int_{-\infty}^t \Pi'_e(t-t')X(t')dt' + \chi_e(t). \quad (19)$$

This equation looks different from Eq. (17). Firstly, it has a memory kernel. The reason is that we do not have the clear time scale separation between the system and environment any more. Secondly, the velocity dependence is absent. Actually, we can do an integration-by-part over t' to the first term on the right hand side. This transforms the dependence on $X(t')$ to $\dot{X}(t')$, and introduces an extra term that renormalizes the potential felt by the nuclei[33]. The renormalization is absent in the adiabatic expansion, since it is included in the Born-Oppenheimer force $F_e(X)$. This difference between the x and \dot{x} expansions is well-known as discussed in Ref. [62]. We will return to the χ_e -correlation function later.

The advantage of the small- x expansion is that, one can make the harmonic approximation for the nuclear dynamics. Many interesting effects can be identified even within this simple approximation, and their key features can be more easily analyzed. This is shown in Sec. 3.

2.4. Including phonon environment

If the system furthermore couples linearly to a phonon environment (either in x or \dot{x}), a SGLE of the same form as Eq. (17) or (19) can be obtained. Altogether, each term at the right side of the two equations will now include terms from electron and phonon, respectively. For example, Eq. (19) changes to

$$\ddot{X}(t) - F_I(X(t)) = - \int_{-\infty}^t \Pi'(t-t')X(t')dt' + \chi(t), \quad (20)$$

with $\Pi' = \Pi'_e + \Pi'_{ph}$, and $\chi = \chi_e + \chi_{ph}$. The first term on the right hand side includes both renormalization and dissipation. The matrix $\Pi'(t-t')$ is the retarded self-energy due to system-environment coupling in the nonequilibrium Green's function (NEGF) theory. This connection with the NEGF theory is very favorable in terms of numerical calculation of realistic systems, since the NEGF theory has been widely used in the study of transport problems. The phonon part Π'_{ph} can be obtained exactly if the system-environment coupling is linear. On the other hand, it is difficult to obtain the electronic part Π'_e exactly. The simplest approach is to take the lowest order term, corresponding to the polarization-like bubble diagram of the self-energy evaluated using the unperturbed electron Green's function. The

correlation function of the fluctuating force χ can also be written in terms of the self-energies in NEGF theory. In equilibrium, they are related through the celebrated fluctuation-dissipation theorem.

We have the following comments on the SGLE: (1) The SGLE is a powerful tool to study MD within electron and phonon environments. Since it is derived from *first-principles*, it can be readily used to study realistic systems. Given the system Hamiltonian, the parameters entering the equation can be calculated and no fitting parameters are needed. (2) Since the environment DoF are noninteracting and treated fully quantum mechanically, the quantum statistics of the environment is taken into account. The environments DoF fulfill the corresponding Fermi-Dirac or Bose-Einstein distribution for electrons or phonons, respectively. This is important at low temperature. (3) The environment is not required to be in equilibrium. When including the electronic environment, we can use it to perform MD in the presence of electrical current. This is the focus of this review. The SGLE can also be used to study phonon thermal transport by introducing two phonon reservoirs at different temperatures. It has been shown for harmonic systems to reproduce the quantum mechanical results exactly[107]. While at high enough temperature, the system behaves classically, and the SGLE gives correct classical results. (4) The memory kernel in Eq. (20) makes numerical simulation quite expensive. Numerical methods have been introduced to eliminate the memory kernel by introducing auxiliary variables[15, 16, 34, 35, 60, 68, 108, 109].

3. Theoretical Analysis: Harmonic modes coupling to electrons

In this section, staying in the harmonic approximation, we analyze the SGLE in different circumstances. We show that, it can describe a varieties of interesting effects. Especially, it has been used to study current-induced dynamics in model systems[82–85, 93, 94, 98, 106]. The nonequilibrium nature of the electronic environment brings in several new effects that are absent in equilibrium, among which are the modification of nuclear potential[95, 96, 110, 111], appearance of non-conservative current-induced forces and effective magnetic field due to the Berry phase of electrons[87, 88, 90, 92–94, 98, 112, 113]. These current-induced effects show up already in the linear coupling regime. Thus, it is convenient to use Eq. (19), and perform mode analysis in the frequency domain. Equation (19) transforms to

$$-\omega^2 X(\omega) = -KX(\omega) - \Pi_e^r(\omega)X(\omega) + \chi(\omega), \quad (21)$$

where K is the dynamical matrix in the harmonic approximation. The equation can be solved for $X(\omega)$. But, here instead of solving it, it is useful to analyze the structure of Π_e^r . To this end, we split Π_e^r into four different contributions

$$\Pi_e^r = \text{Re}\Pi_{e,sym}^r + \text{Re}\Pi_{e,asym}^r + i\text{Im}\Pi_{e,sym}^r + i\text{Im}\Pi_{e,asym}^r. \quad (22)$$

The real part $\text{Re}\Pi_e^r$ has a symmetric $\text{Re}\Pi_{e,sym}^r$ and an anti-symmetric $\text{Re}\Pi_{e,asym}^r$ part in the vibrational mode index. The imaginary part $\text{Im}\Pi_e^r$ is similar. The two anti-symmetric parts are nonequilibrium contributions and are zero in equilibrium. In the following, we analyze these terms one by one.

3.1. Electronic friction

Electronic friction comes out of the adiabatic expansion as the first order correction yielding Γ_e in Eq. (17). This dissipative force leads to energy transfer between the electrons and the nuclei, thus is beyond the Born-Oppenheimer approximation. This energy transfer plays an important role in adsorbate dynamics on metal surface[79, 114–120]. In our harmonic model with small- x expansion, the third term in Eq. (22) describes the electronic friction felt by the nuclei. From it, we can define a frequency-dependent, non-Markovian $\Gamma_e(\omega) = \text{Im}\Pi_{e,sym}^r(\omega)/\omega$. Its diagonal elements represent effective broadening of vibrational modes and are related to the vibrational lifetime.

Physically, the electronic friction originates from excitation of EHP in the Fermi sea by nuclear motion. It has been derived using different theoretical approaches[54–56, 81–83, 85, 87, 93]. One notable example is that of Head-Gordon and Tully [79–81]. By deriving the nonadiabatic coupling between electronic states and applying GLE and mean-field theory, they calculated the electronic friction for the CO/Cu(100) system. This approach has now become a standard tool in the study of adsorbate dynamics on metal surface, even under external driving. Recently, the tensorial and mode-specific feature of the friction matrix in energy transfer has been analyzed which we return to later[50, 51], and the similarities and differences of different definitions have also been discussed[54].

The electronic friction we derived here also applies to the nonequilibrium case, i.e., in the presence of electrical current. The electronic density of states (DOS) determines directly the magnitude of the electronic friction. If the

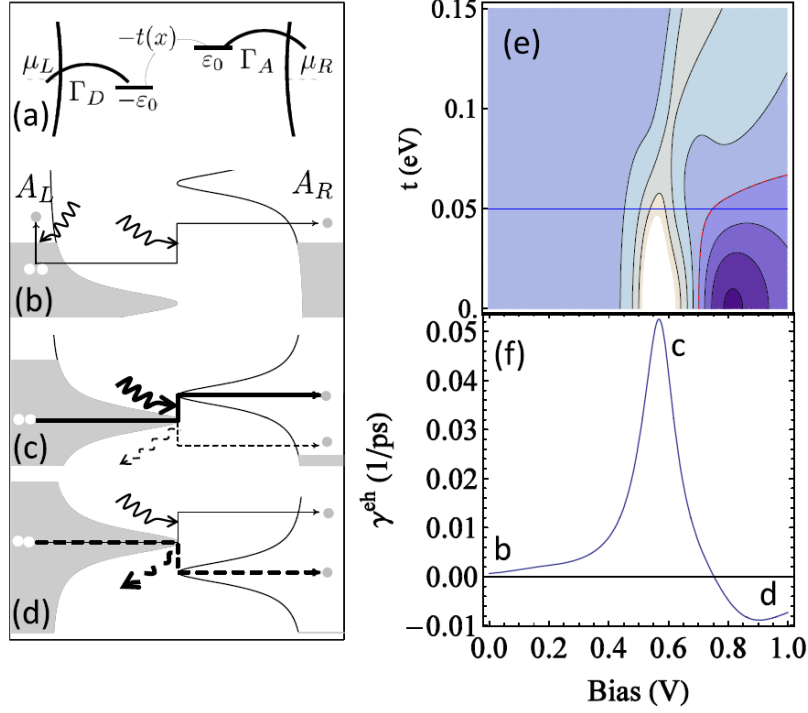


Figure 1: (a) Schematics of the a donor-acceptor system coupling to a vibrational mode, whose displacement is denoted by x . The donor and acceptor couples to the left and right electrodes, respectively, with broadening parameter Γ_D and Γ_A . (b) Typical EHP excitations at zero bias. Intra-electrode excitation in the left electrode and inter-electrode excitation from the left to the right electrode are shown. Similar excitation in the right electrode and from the right to left are also present, but not shown here. (c) Finite bias, resonant absorption of the vibration. This corresponds to c in (f), where the electronic friction is maximum. (d) Finite bias, resonant emission of the vibration, corresponding to the d in (f). The electronic friction becomes negative. (e) Contour plot of the electronic friction as a function of bias and hopping element t between the donor and acceptor site. The red line separates the negative from the positive friction region. (f) A line cut of (e) at $t = 0.05$ eV. Figure adopted from Ref. [88] with permission.

electronic DOS around the bias window is flat, we can neglect its energy dependence. In this case the bias dependence of the electronic friction will be negligible corresponding to the wide band limit in quantum transport. In the opposite case, the bias dependence becomes important and new effect may emerge. In Ref. [88], the authors considered a single vibrational mode coupling to a donor-acceptor two-level electronic system (Fig. 1 (a)). For this single mode model quantities in Eq. (17) are all numbers. The bias dependence of the electronic friction γ_e can be expressed from the rates of vibrational emission (\mathcal{B}) and absorption (\mathcal{A}) processes, see Fig. 1(b)-(f),

$$\gamma_e = \mathcal{A} - \mathcal{B}. \quad (23)$$

Depending on the relative position of the donor and acceptor level, there could be resonantly enhanced emission or absorption of the vibrational mode. For resonant absorption, $\mathcal{A} > \mathcal{B}$, and γ_e is large (Fig. 1 (c)), while for resonant emission γ_e decreases and even goes negative (Fig. 1 (d)). In the former case, the donor level is lower than the acceptor level by one vibrational quantum Ω and the main transport channel is accompanied by vibrational absorption. Thus, the current can be used to depopulate the vibrational mode, leading to current-induced cooling of the mode. On the other hand, in the latter case, the position of the two levels are reversed. This population inversion is akin to the case of the mode populations in a laser. This vibrational amplification by stimulated emission is the physical reason that leads to the negative electronic friction. This negative friction is a nonequilibrium effect, contrary to equilibrium, where the relative magnitude of \mathcal{A} and \mathcal{B} is determined by the detailed balance relation $\mathcal{B}/\mathcal{A} = e^{-\Omega/k_B T} < 1$, resulting in a positive friction. The anharmonic effect on heating and cooling of the molecular junction has been analyzed by

Segal and coauthors[121].

In our theory, we have ignored the effect of electron-electron interaction on the electronic friction beyond the adiabatic mean-field screening of the coupling. Combined with numerical renormalization group calculation, Dou *et al.*[56] studied the modification of electronic friction due to strong electron-electron correlation through the Anderson-Holstein model. They found a qualitative difference of the electronic friction calculated from the numerical renormalization group (NRG) and the dynamical mean field theory (MFT) (Fig. 2). This highlights the importance of electron correlation on the electronic friction.

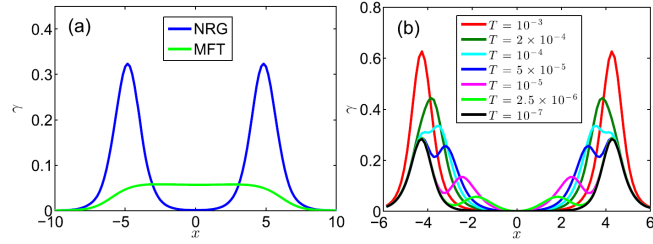


Figure 2: Calculation of electronic friction γ of an Anderson-Holstein model. (a) Electronic friction γ as a function of position x using the numerical renormalization group (NRG) and mean field theory (MFT) calculations. Note that MFT fails to recover two peaks in the friction. (b) Electronic friction according to NRG theory at low temperature; note that the two peaks in friction split into four peaks at low temperature. Figure adopted from Ref. [56] with permission.

3.2. Joule heating from the nonequilibrium fluctuations

The interaction of the flowing current with the nuclei leads to heat transfer from the electronic to the nuclear DoF, normally termed Joule heating. In the SGLE, this is reflected in the correlation function of the fluctuating force. In equilibrium, we have the fluctuation-dissipation relation

$$\langle \chi_e(\omega) \chi_e^*(\omega) \rangle_{\text{eq}} = -\text{Im} \Pi_e^r(\omega) \coth(\omega/2k_B T). \quad (24)$$

This includes both thermal and quantum fluctuations. In nonequilibrium, the correlation function of χ_e gains an extra term due to the voltage bias. In the wide band limit, it has a bias and energy dependence as

$$\delta \langle \chi_e(\omega) \chi_e^*(\omega) \rangle \propto (eV - \omega) \Theta(eV - \omega). \quad (25)$$

The extra noise is linear in ω . The Heaviside step function $\Theta(eV - \omega)$ means that, due to energy conservation, the extra noise have an upper limit determined by the applied bias. Fitting the nonequilibrium noise correlation function to a form similar to Eq. (24), we can define an effective electronic temperature of a given vibrational mode i in the presence of current flow,

$$\langle \chi_{e,i}(\omega) \chi_{e,i}^*(\omega) \rangle_{\text{neq}} = -\text{Im} \Pi_{e,ii}^r(\omega) \coth(\omega/2k_B T_{\text{eff},i}). \quad (26)$$

It should be noted that, the above equation contains the electron-nuclear coupling terms and different modes will generally experience different effective electronic temperatures. From this analysis, Joule heating can be understood from another point of view. The applied bias changes the effective temperature of the electronic system and the temperature difference leads to heat flow between the electrons and the nuclei.

It can be shown analytically that, for harmonic oscillators, using the above noise correlations, the prediction of Joule heating from the SGLE is equivalently to that from the NEGF method under the same approximations[90]. That is, it can produce fully quantum mechanical results for harmonic oscillators.

3.3. The non-conservative and effective Lorentz force

When a current flows through a conductor, it induces forces on the nuclear DoF. Whether this current-induced force is conservative or not is a question that brought some confusion[122–125]. Todorov and co-authors gave a concise answer to this question[126–128]. Moreover, they showed that the non-conservative force can be used to

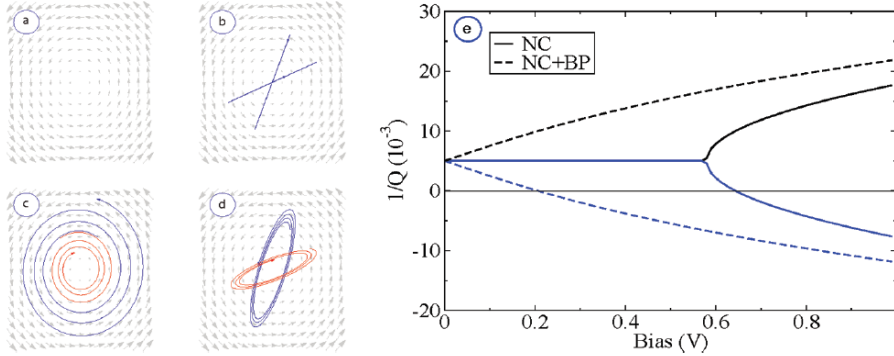


Figure 3: (a) Schematics of the force field generated by the non-conservative current-induced forces. (b) Trajectories of two linear harmonic oscillators without non-conservative forces. (c) Trajectories in the presence of non-conservative forces. The amplitude of the red mode damps with time, while that of the blue mode grows with time, indicating an instability. (d) When both the non-conservative and the Lorentz force are present, the trajectories changes. (e) Inverse Q factor of the two modes as a function of bias in the presence of non-conservative (NC) or Lorentz (BP) force. Negative $1/Q$ means instability indicated in (c) and (d). Figure adopted from Ref. [87] with permission.

drive an atomic motor using Ehrenfest MD to perform the numerical calculations[126, 129]. Later on, the SGLE was used to study the same problem[87], and the effect has been extended to mesoscopic systems[93, 113, 130–132]. It has the advantage of considering the deterministic current-induced forces and stochastic Joule heating on an equal footing[87, 90, 93, 94, 106]. It was here predicted that, in addition to the non-conservative force, there is an extra effective Lorentz force originating from the Berry phase of the electrons. We discussed how the Joule heating can be considered within the SGLE in Subsec. 3.2 in terms of stochastic forces, while here we focus on the deterministic current-induced forces.

Firstly, the force contributed from $F_{nc} \equiv -\text{Re}\Pi_{e,asym}^r \dot{X}$ is non-conservative. This can be seen from the anti-symmetric properties of $\text{Re}\Pi_{e,asym}^r$, which leads to $\nabla \times F_{nc} \neq 0$. This means, the nuclei move within a non-conservative force field (Fig. 3 (a)). If they move along a certain loop, F_{nc} can pump or extract energy from the nuclei depending on the direction of the motion (Fig. 3 (c, d)). This energy transfer through deterministic work is fundamentally different from Joule heating. Since the off-diagonal (anti-symmetric) part of $\text{Re}\Pi_{e,asym}^r$ is important, the system should have at least two DoF.

Secondly, the force contributed from $F_{bp} \equiv -\text{Im}\Pi_{e,asym}^r \dot{X}$ is different from friction. Its effect on the nuclear dynamics is similar to that of a magnetic field, due to the anti-symmetric property of $\text{Im}\Pi_{e,asym}^r$. It originates from the Berry phase of the electrons, which back acts on the nuclei. Actually, this force is more easily understood from the adiabatic expansion. It, together with the friction, comes as the first order correction in the expansion ($-\Gamma_e \dot{X}$ term in Eq. (17)). We should mention that the Berry phase comes from the time-reversal symmetry breaking in the electronic environment, and becomes zero in equilibrium. This phase is not quantized, and F_{bp} changes continuously with the applied voltage. Berry and Robbins have studied this kind of ‘geometric magnetism’ and showed that it is zero when the system has a discrete spectrum[133]. Here, the coupling of the system to the electronic environment leads to broadening of the spectrum, and renders the Berry phase non-zero. Like the Lorentz force, F_{bp} does no work on the nuclei, but it changes the orbit of the eigen mode motion. It may change the orbit from linear to elliptical (Fig. 3), and help the non-conservative force to do work on the nuclei.

Both F_{nc} and F_{bp} come into play only when there are at least two DoF in the system. Thus, the main results can be illustrated by a two-mode model[87, 90]. Neglecting the fluctuating forces first, we can write their equations of motion in the eigen mode basis

$$\begin{pmatrix} \ddot{x} \\ \ddot{y} \end{pmatrix} = - \begin{pmatrix} \omega_1^2 & a \\ -a & \omega_2^2 \end{pmatrix} \begin{pmatrix} x \\ y \end{pmatrix} - \begin{pmatrix} \gamma & b \\ -b & \gamma \end{pmatrix} \begin{pmatrix} \dot{x} \\ \dot{y} \end{pmatrix}. \quad (27)$$

Here, ω_1 and ω_2 are the angular frequency of the two otherwise independent vibrational modes. Their simultaneous coupling to the electrical current leads to indirect vibrational coupling, parametrized by a and b in the above equation.

They represent the non-conservative and the effective Lorentz force, respectively. We can analyze the eigen spectrum of the system including a and b . We find that, above certain bias, the two forces, especially F_{nc} , may drive the system into a run-away instability, characterized by a negative damping corresponding to a negative $1/Q$ factor, as shown in Fig. 3 (e). In this situation the energy of the unstable harmonic mode will keep increasing in time once it is excited. It is also shown that, the change of the orbit by F_{bp} helps F_{nc} to perform work. This is f.ex. seen in how the threshold bias of the instability decreases when including F_{bp} .

3.4. Renormalization of the vibrational potential and bistability

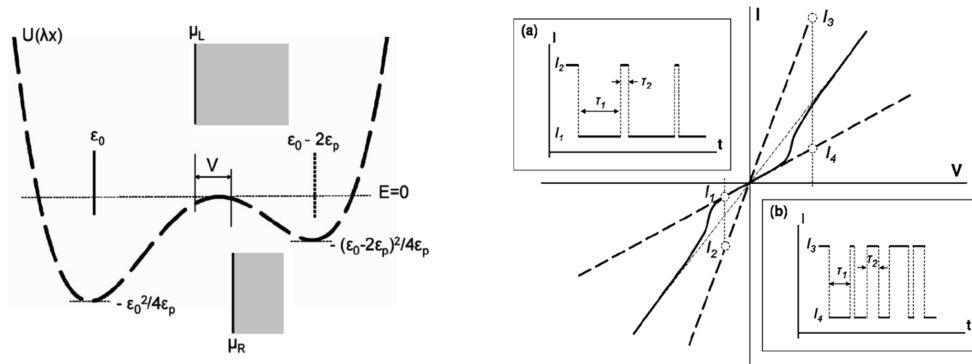


Figure 4: Left: The potential profile of a harmonic oscillator coupling to one single electronic level at finite bias. The single well harmonic potential is modified and acquires a bistable profile at finite bias. Right: The I - V curve of the single level model showing bistability. (a) The temporal dependence of the electrical current at small bias, where the oscillator spends most of the time in a deeper well and occasionally jumps to a shallower well. (b) The same as (a), but at higher voltages. Now the probability to occupy the shallower well, and the switching rate increase due to higher effective temperature. Figure adopted from Ref. [85] with permission.

If the nuclei couple strongly to the electrons, the potential felt by the nuclei may change a lot when there is an applied voltage bias. It may even generate a bistable state and lead to conductance switching behavior. It has been studied within the minimal Anderson-Holstein model[85, 96], where one vibrational mode couples to the electronic system through an onsite interaction. The left part of Fig. 4 shows the voltage induced bistable states. It comes from a harmonic potential at zero bias. The right part of Fig. 4 shows its signature in the electrical current. In Fig. 5, different kinds of behaviors in phase space are also observed at finite biases.

4. Applications

4.1. Numerical implementation

Before turning to the applications of the SGLE, we discuss briefly two technical issues faced in any numerical implementation of the SGLE approach. Firstly, the friction part of the SGLE in general has a memory kernel due to the difficulty in separating completely the time scales of the system and the bath. Although this does not pose a conceptual problem, in practical, realistic calculations, it is numerically more involved compared to a time-local friction. To this end the non-local, non-Markovian equation can be transformed into a local, Markovian one by introducing auxiliary DoF into the equation. This trick has been successfully used by different authors [20, 34]. Secondly, the colored noise spectrum requires certain attention in the generation of the random force. Two approaches have been applied in the literature. This first one makes use of the fact that the noise is δ -correlated in the frequency domain. Thus, generating the noise in the frequency domain and making fast Fourier transform to time domain gives a time-correlated noise that can be used to do the MD simulation[14, 134]. The problem of this method is that, one has to generate the noise and store it before performing the simulation. For large scale simulations involving many DoF this could result in a storage problem. More importantly, for certain applications, i.e. molecular diffusion on, or scattering off, a metal surface, the coupling of the system to the baths may change during the simulation. In this case one needs to adjust the

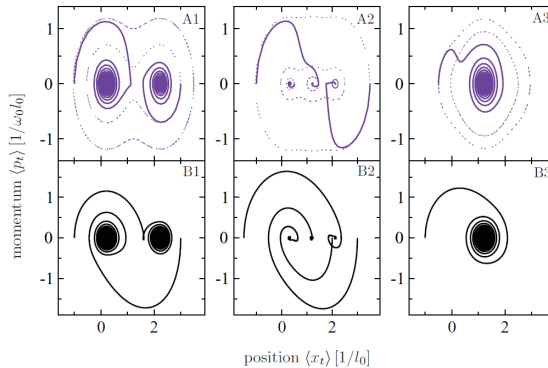


Figure 5: Bias dependent phase space trajectories for a single electronic state coupling to a vibrational mode in the Holstein form. Dashed lines in row A are results from the Born-Oppenheimer dynamics without friction, solid lines include friction. Row B shows results including all the non-adiabatic effects in the SGLE. The voltage bias modifies the number of fixed points and the trajectories drastically. Figure adopted from Ref. [96] with permission.

noise on the fly. To overcome this difficulty, different approaches have been adopted to generate the noise directly in time domain [34, 135, 136].

4.2. Adsorbate dynamics on metal surfaces

The coupling between molecular motion and EHP excitation is important in order to understand adsorbate dynamics at surfaces, F. ex. it was found that the vibrational lifetime of CO on a metal surface is in the order of ps, while on a NaCl surface it is many orders of magnitude longer (ms)[115, 137], see Ref. [138] for a recent review. Detailed theoretical and experimental study shows that the coupling between molecular vibrations and the EHP excitation is key to understand this difference. Molecular-beam surface scattering experiments provide direct evidence of the coupling of molecular motion to the EHP excitation[116, 117, 139–141]. The detection of chemicurrent during the adsorption of molecules on thin metal surface of tunnel junctions is another signature of coupling[118–120]. The electronic friction language was quite successful in understanding these experiments. Head-Gordon and Tully [81] in 1995 developed a method to perform classical MD including electronic friction from metal electrons. By deriving the nonadiabatic coupling between electronic states and applying the GLE, they obtained electronic friction for the CO/Cu(100) system. Since then, generalized Langevin equations has become an important tool in the study of adsorbate dynamics on metal surface, even under external driving.

Although the general picture discussed above is widely accepted, obtaining quantitative measures of the role of EHP excitation in the adsorption and reaction dynamics is still challenging. Here, we only summarize recent theoretical and experimental advances in typical systems[41–43, 47–56, 142–146].

Bünemann *et al.* studied inelastic H-atom scattering from Au(111) surface[46]. A beam of nearly mono-energetic H atoms was prepared by laser photolysis and injected on to Au(111) surface with and without adsorbed Xe layers. The experimental setup allowed study of inelastic H-atom scattering with different incidence and scattering angles. The experimental results show drastic difference between Xe and Au surface scattering. For Xe surface, due to the requirement of energy and momentum conservation, the translational energy loss of the H-atom was small. For Au(111) surface, the translational energy of H-atom can be directly converted to EHP excitations. Thus, the energy loss was much larger than in the Xe surface case. The experimental results were compared to theoretical simulations with and without including the electronic friction (Fig. 6), and it was seen how the electronic friction was needed to obtain a reasonable agreement with the experimental results. This work shows clear evidence of translational energy dissipation due to electronic friction.

The tensorial feature of Γ_e matrix in Eq. (17) was emphasized in recent works[50, 51]. The off-diagonal elements of Γ_e in the mode space couple different modes together and influence the energy distribution within different vibrational modes. The electronic friction is normally anisotropic, i.e., depending on the direction in real space and having different magnitude for different vibrational modes. Figure 7 shows an example of CO adsorbed at an atop site of

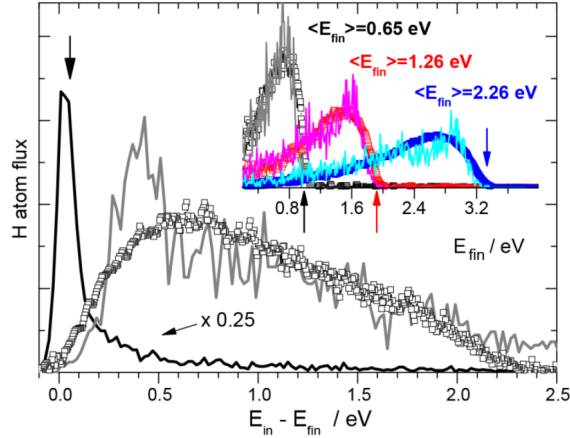


Figure 6: Comparison of the experimentally obtained kinetic energy loss spectrum to theoretical simulations. Theoretical energy loss found when neglecting (solid black line), and including (solid gray line) electronic excitation. Experimental energy loss for $E_{in} = 2.76$ eV is shown as open squares. The vertical arrow marks the expected energy loss for a binary collision between an H and an Au atom. The inset shows the incidence energy dependence, E_{in} , of the experimentally derived translational inelasticity (open squares) and comparison to theory (solid lines): $E_{in} = 3.33$ eV (blue), 1.92 eV (red), and 0.99 eV (black). Colored arrows mark the three incidence energies. Also shown are the average final translational energies, $\langle E_{fin} \rangle$. The scattering angles are $\theta_i = 45^\circ$, $\theta_s = 45^\circ$, and $\phi_i = 0$ with respect to the [101] direction. In all cases, the scattered H atoms remain unthermalized with the solid, emerging with a substantial fraction of their incidence translational energy. Figure adopted from Ref. [46] with permission.

Top View $\begin{matrix} y \\ z-x \end{matrix}$	Side View $\begin{matrix} z \\ y-k \end{matrix}$	Mass-weighted Friction Tensor in ps^{-1}					
Equilibrium Atop		C_x	C_y	C_z	O_x	O_y	O_z
		0.248	0	0	-0.088	0	0
		C_y	0.248	0	0	-0.088	0
		C_z		0.245	0	0	-0.077
		O_x			0.032	0	0
		O_y				0.032	0
		O_z					0.034
Non-equilibrium Tilted		C_x	C_y	C_z	O_x	O_y	O_z
		0.248	0	0	-0.085	0	-0.011
		C_y	0.248	0	0	-0.085	-0.011
		C_z		0.245	0.021	0.021	-0.075
		O_x			0.040	0	0
		O_y				0.040	0
		O_z					0.034

Figure 7: CO on top of Cu(100) surface. (left) CO adsorbed at an atop site of a Cu(100) surface in the equilibrium position and a nonequilibrium tilted geometry as viewed from xy (top view) and yz (side view) planes. (right) Mass-weighted friction tensor (in ps^{-1}) for the two geometries. The coloring scheme is consistent for x (red), y (green), z (blue), xz (purple), and yz (brown) components of the friction tensor. Components smaller than 0.002 ps^{-1} are set to zero. Figure adopted from Ref. [50] with permission.

Cu(100) surface. The friction matrix elements in real space are shown. Based on this understanding, Maurer *et al.* studied the scattering and dissociative chemisorption of H_2 on the Ag(111) surface (Fig. 8). Although the electronic friction only accounts about 5% of the energy loss, the anisotropy of the friction induces dynamical steering that changes the reaction outcomes.

Irradiation of a metal with an ultrafast femtosecond laser pulse induces electronic excitations and adsorbate desorption from the metal surface. This probes how hot excited electrons transfer energy to the adsorbate vibrations. The Langevin equation has been used to study these processes[144, 147]. Figures 9 and 10 show two examples of simulations after laser excitation.

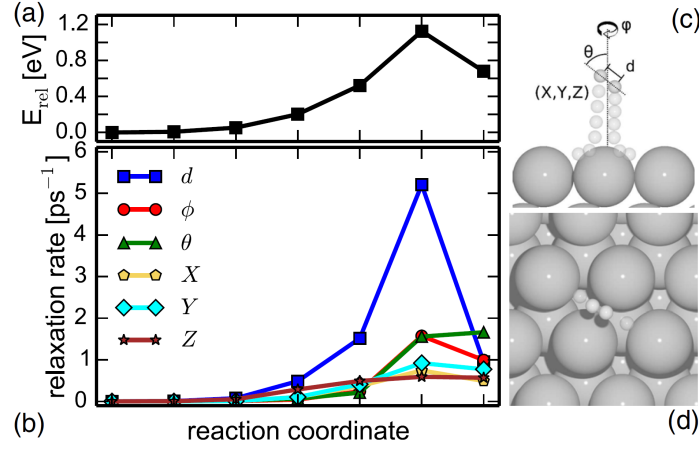


Figure 8: H₂ on top of Ag(111). (a) Relative energy along a minimum energy path (MEP) of H₂ dissociation on Ag(111). The path is shown in (c) and (d). (b) Relaxation rates in ps⁻¹ obtained from the diagonal elements of electronic friction tensor in internal coordinates: bond stretch d , azimuthal angle ϕ , polar angle θ , and the three Cartesian center of mass coordinates of the hydrogen molecule (X, Y, Z). Off-diagonal elements (not shown) can modify relaxation rates by 30% or more. (c) Side view of the dissociation along the minimum energy path. (d) Top view of start and end point of MEP. Figure adopted from Ref. [51] with permission.

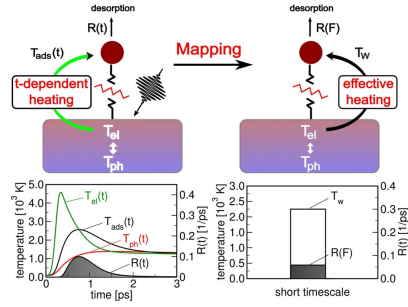


Figure 9: Desorption of D₂ from Ru after excitation with a 130 fs Gaussian laser pulse at 800 nm, $F = 140$ J/m². Left panel: time-dependent behavior of the electron, phonon, and adsorbate temperatures (T_{el}, T_{ph}, T_{ads}). Right panel: the hot electron-mediated dynamics is mapped to an effective heating mechanism similar to Eq. 26. T_w represents an effective temperature that captures the physics of the adsorbate excitation, and the fluence F is related to the temperature T_w . T_w determines the microscopic properties of the desorbed molecules, and it's of great benefit to numerical simulation. Figure adopted from Ref. [147] with permission.

4.3. Joule heating and current-induced forces in molecular conductors

One advantage of the SGLE is that it allows consideration of Joule heating and current-induced forces on an equal footing. The authors in Ref. [92] studied the interplay of these two channels of energy transfer from the nonequilibrium electronic to the nuclear DoF. The coupling of the system to phonons and electrons in the two electrodes was considered simultaneously. It was found that, the effect of the current-induced force depends on the direction of the current flow. In particular, for a symmetric system with current flow, a asymmetrically placed hot-spot in the nuclear energy distribution (Fig. 11) was observed. This effect mainly comes from the non-conservative part of the force and depends on the wave length of the electron scattering states. These results show the important role played by the non-conservative current-induced force and its relation to the momentum transfer from charge carriers to the nuclear DoF[128]. Asymmetric heating has been observed in nanojunctions. These effects are central for the directed motion of atoms in the electromigration of nanojunctions[148, 149].

Our analysis so far is limited to the harmonic approximation for the vibrations. In the SGLE, the anharmonic interactions is taken into account classically. Direct MD simulation using either Eqs. (17-20) takes the anharmonic

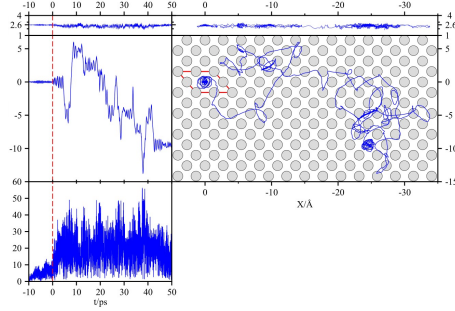


Figure 10: Time evolution of a typical trajectory of a single CO molecule on Ru(0001) surface from MD with electronic friction, starting from its global minimum, i.e., on top of a Ru atom ($X = Y = 0$, $\theta = \phi = 0$), when driven by hot electrons generated from a 140 J/m^2 laser pulse (at $t = 0$), $\lambda = 400 \text{ nm}$, FWHM = 50 fs, and base temperature 300 K. The top and middle left panels show the center of mass coordinates Z and Y over time, the top right and middle panels the entire trajectory in the (X,Z) and (X,Y) planes, respectively. The lower left panel gives the tilt angle θ as a function of time. The top Ru is visualized with gray circles. Figure adopted from Ref. [144] with permission.

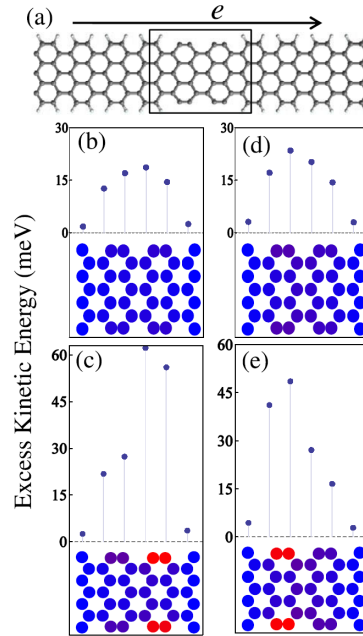


Figure 11: (a) Structure of a partially passivated armchair graphene nanoribbon. The atoms in the solid square couple to a nonequilibrium electronic reservoir. (b)-(c) The excess kinetic energy of each atom without and with the current-induced non-conservative and Lorentz force. The voltage bias is $V = 0.4 \text{ V}$, the temperature is $T = 300 \text{ K}$, and the Fermi energy $E_F = 1.4 \text{ eV}$. (d)-(e) Same as (b)-(c), but at $E_F = -1.0 \text{ eV}$. Figure adopted from Ref. [92] with permission.

vibrational interactions into account in the same way as the classical MD. But the inclusion of zero point motion and correct quantum distributions in the SGLE extends its range of validity to the study of heat transport at low temperature and dynamics in the presence of electrical current.

In Ref. [93], Bode and co-authors considered anharmonic atomic dynamics driven by an electrical current using an equation similar to Eq. (17). There, the anharmonicity comes from the adiabatic F_e , which depends on the atomic displacement X . They found that, beyond the harmonic instability, the anharmonic forces stabilize the dynamics and the system goes into some kind of limit cycles. The appearance of the limit cycles can be seen from the two-peak to one-peak transition in the current and displacement correlation functions (Fig. 12 (c), (d)).

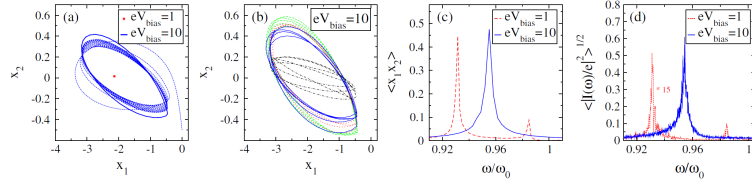


Figure 12: Results from a model-system consisting of two vibrational modes coupling to two electronic levels in the scattering region going beyond the harmonic approximation. (a) Limit cycle (blue solid line) and its approach (blue dotted line) at large bias vs stable oscillations at low bias (red asterisk) from the Langevin dynamics without fluctuating force. (b) Several periods of typical trajectories with fluctuating forces for the parameters of the limit cycle in (a). (c) Fourier transform of the correlation function $\langle X_1(t)X_2(t + \tau) \rangle$. The limit cycle is signaled by a single peak, as opposed to two peaks in the absence of a limit cycle. (d) The same signature appears in the current-current correlation function, making the onset of limit-cycle dynamics in principle observable in experiment. Figure adopted from Ref. [93] with permission.

The SGLE has also been used to study current-induced dynamics going towards a more realistic atomistic description of the system. The authors have considered the dynamics of an carbon atomic chain between two graphene nanoribbon electrodes[89, 91, 150, 151]. A tight-binding model for the electronic structure and the Brenner potential for the inter-atomic interaction was used. The electronic structure was updated on the fly during the MD simulation (Fig. 13). This kind of calculation makes it possible to study current-induced dynamics using MD simulation. So far, the dynamics was based on empirical potentials. However, it would be highly desirable to perform *at initio* MD based on f.ex. DFT electronic structure calculations. In order to achieve this goal, an efficient way of performing the DFT calculations is crucial possibly including partly the non-equilibrium forces using DFT-NEGF[152].

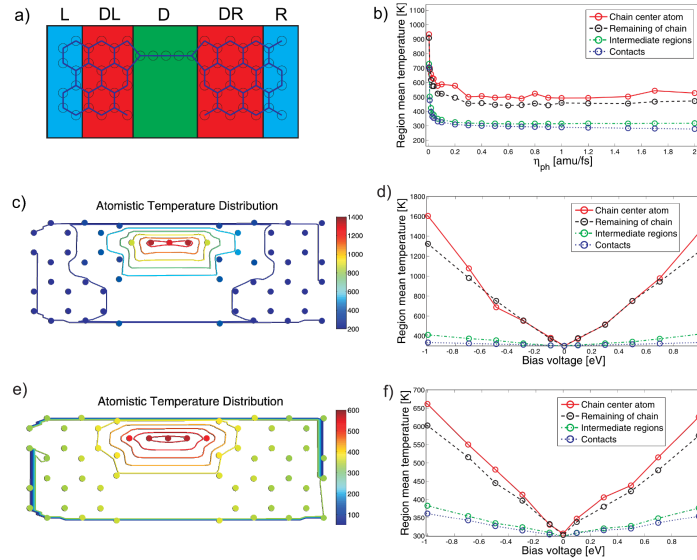


Figure 13: (a) The system considered in the calculation, with single atomic carbon chain between graphene nanoribbon electrodes. (b) Temperature obtained from the atomic kinetic energy as a function of phonon friction. (c-d) Obtained temperatures deduced from the atomic kinetic energy of different atoms within the harmonic approximation. (e) The simulations were run at $T = 300$ K and at $eV_b = 1$ eV. (d) The atomic temperature as a function of bias at $T = 300$ K. (e, f) Corresponding atomistic temperature distributions including the anharmonic interactions. The anharmonic interactions redistribute part of the energy from the modes in the chain to the bulk modes in the lead. Figure adopted from Ref. [89] with permission.

4.4. Nuclear quantum effect in molecules and solids

The nuclear quantum effect (NQE) has important implications for the physical and chemical properties of molecules and crystals made from light elements and stiff chemical bonds[153]. One notable example is the complicated behav-

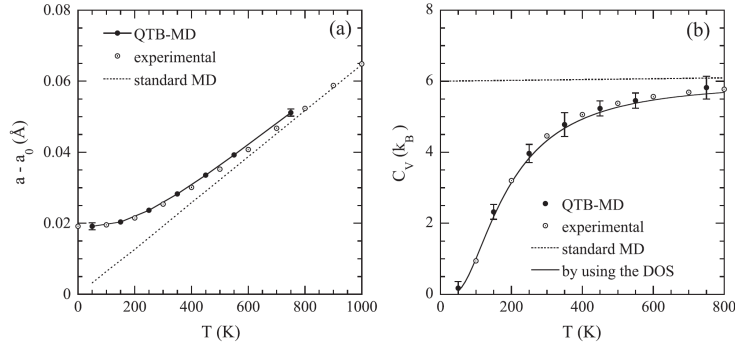


Figure 14: MgO crystal parameters predicted from MD with QTB (QTB-MD). (a) Temperature dependence of the lattice parameter a . The a_0 value is obtained by extrapolating, to 0 K, the linear behavior observed at high temperature. The QTB-MD reproduces the experimental data at low temperatures. (b) Temperature dependence of the heat capacity per molecule C_V . The QTB values (obtained by differentiation of the mean energy) agree with the experimental data and the results derived using the harmonic density of vibrational states (DOS). The standard MD simulation gives reliable values only at temperatures higher than the Debye one (940 K). Figure adopted from Ref. [18] with permission.

ior of the hydrogen bond under different conditions[154]. To study the NQE, the dynamics of nuclei has to be treated quantum mechanically, and to this end path-integral MD (PIMD) and Monte Carlo methods are normally used. Recently, the semi-classical Langevin equation was used to partially account for the nuclear quantum effect[17–25]. The idea is to simply attach one *artificial* quantum thermal bath (QTB) to each nuclear DoF. For each element X_i , we have

$$\ddot{X}_i - F_{I,i} = -\gamma_i \dot{X}_i + \chi_i. \quad (28)$$

Equation (28) has similar form as Eq. (17). Its left side represents the original equation of motion. Different from Eq. (17) where the system couples to an electron bath, in Eq. (28) X_i couples to an *artificial* QTB. The friction coefficient, γ_i , is an adjustable parameter, and the correlation function of the fluctuations fulfills the fluctuation-dissipation relation: $\langle \chi_i(\omega) \chi_i^*(\omega) \rangle = \gamma_i \omega \coth(\omega/2k_B T)$. This is a colored noise spectrum that depends on ω . In the high temperature limit, it reduces to the well-known relation: $\langle \chi_i(\omega) \chi_i^*(\omega) \rangle = 2\gamma_i k_B T$, where ω -dependence can be ignored and the noise spectrum becomes white.

The advantages of this approach is that it introduces almost no extra computational cost compared to standard classical MD. Its performance in determining many physical properties has been calibrated through comparison to the fully quantum mechanical approaches[17, 18, 21, 23–25, 155, 156].

Dammak *et al.* showed that temperature dependence of MgO’s lattice constant and its heat capacity calculated from the SGLE agree well with experimental measurements[18](Fig. 14). Bronstein and coauthors studied the NQE on the phase transition in pure and salty ice at high pressure[24, 25]. They found excellent agreement between the experimental and the theoretical results using the QTB model. Further applications include vibrational properties of polyatomic molecules [157, 158], isotope effect[19], shocked-compressed molecules[159, 160], spin-phonon dynamics[161–163].

Ceriotti *et al.* took an important step further[17, 20, 22, 23, 68, 70, 164]. We have mentioned that, given the full Hamiltonian of the global system, the parameters entering the SGLE are derivable from the microscopic Hamiltonian. Ceriotti and coauthors have performed a ‘reverse-engineering’ of the QTB, making full use of the flexibility in choosing the bath parameters for target applications. This concept has been termed ‘Langevin thermostat *à la carte*’. They showed that through systematic optimization, the properties of the QTB can be tailored to display desired sampling features, i. e., selective coupling of the thermal bath to target certain vibrational modes. When combined, the QTB can significantly improve the convergence and scalability of PIMD to reach a performance comparable to that of the standard Nosé-Hoover chain thermostat.

As a semi-classical approach, the SGLE can only account partially for the quantum effects. More importantly, it has the problem of zero point energy (ZPE) leakage [165]. This problem arise from the fact that in the SGLE, the ZPE is stored in each harmonic mode classically. In the presence of anharmonic couplings, even at zero temperature, the classically stored ZPE can redistribute between different vibrational modes. This unphysical energy flow from the

high frequency modes to the low frequency vibrational modes results in a wrong energy distribution (ZPE leakage). The average energy of each vibrational mode is determined by its coupling to the thermal bath characterized by γ in the Langevin equation and to other modes determined by the anharmonic coupling. The problem is common to methods based on classical trajectories. Different solutions of this problem have been proposed[21, 165, 166]. Briec *et al.* have studied this effect carefully in both model and realistic structures[21] and found that, in most cases, by simply increasing γ , the energy exchange between the thermal bath and the vibrational mode becomes dominant. In this way the ZPE leakage becomes relatively small. Taking notice of this problem, except for very anharmonic systems, the QTB can then give reasonable results for many properties.

4.5. Quantum thermal transport in nanostructures

By attaching the system to multiple QTBs, one may study phonon heat transport using the SGLE[12–16, 30–32, 36, 37]. For linear harmonic systems, the ZPE leakage is not present, and has been shown analytically that, the SGLE produces exact results consistent with fully quantum mechanical approaches (Fig. 15)[14, 27, 29]. Figure 15 compares numerically the thermal conductance of a model harmonic chain calculated from the SGLE and the NEGF method. The agreement is due to the quantum statistics of the mode occupations in the thermal bath. For linear harmonic systems this can efficiently propagate into the system through the system-bath coupling. This is especially important for systems with light atoms whose Debye frequency is high, and classical statistics fails. For example, the room temperature thermal conductivity of carbon materials can not be predicted directly from classical MD due to the large Debye frequency. Similarly, Langevin equations for electrons are also derived and shown to be consistent with the standard Landauer or NEGF result for noninteracting electrons[27, 32].

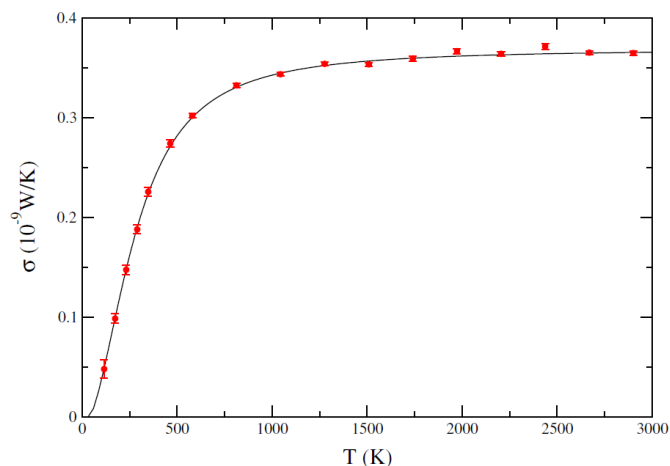


Figure 15: Thermal conductance σ as a function of temperature for a 1D harmonic chain with on-site potential. The solid line is the NEGF result, while the symbols are MD results. They agree with each other. Figure adopted from Ref. [14] with permission.

On the other hand, including the anharmonic interactions, at high temperatures where the quantum mechanical effect is not important, the SGLE yields results consistent with classical MD simulation[14]. Thus, the transition of heat transport from quantum, ballistic to the classical, diffusive regime can be studied using this approach[14, 31, 33, 167]. Figure 16 shows the thermal conductance (σ) of a graphene nanoribbon as a function of ribbon length. When the ribbon is short, σ does not depend on the length, the system is in the ballistic transport regime. When the length is > 600 nm, σ decreases with length as $\sim L^{-0.67}$ [33].

Intuitively, the ZPE leakage is not expected to have a large influence on the real space heat transport. The modes contributing most to heat transport should be traveling waves that are delocalized in real space. Thus, the energy leakage between different modes does not take place locally, while the heat current is calculated locally. But a case study shows the opposite. A comparison of classical, semi-classical and experimental results of thermal conductivity of solid argon shows that, the SGLE approach behaves much worse than the classical MD [165]. Presumably, the

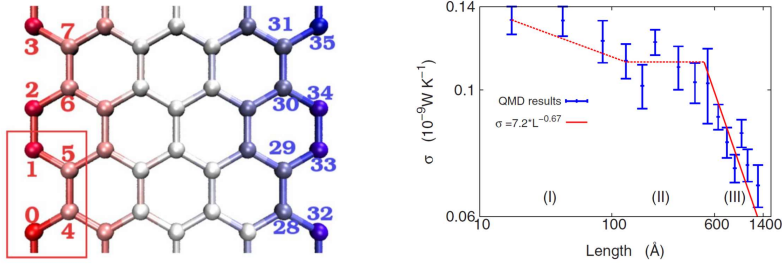


Figure 16: Left panel: The structure for an armchair graphene strip. The box (red) is the unit cell. The length of the ribbon along transport direction (horizontal direction) is varied while keeping the average temperature at 300 K, while periodic boundary condition is applied to the perpendicular direction. Right panel: The dependence of the thermal conductance on the length of the system at 300 K in logarithmic scale. Phonon transport changes gradually from ballistic to diffusive with increasing length of the system. Figure adopted from Ref. [33] with permission.

failure of the SGLE is due to the ZPE leakage, while the accidental cancellation of the two errors makes the classical MD results agree better with the experiments. This clearly shows the limitation of the SGLE, but more careful studies are needed before one can draw any conclusions on the effect of ZPE leakage on the thermal conductivity predicted from the SGLE.

One important advantage of the GLE approach is that it is a *first principles* approach, in the sense that the parameters entering the SGLE can be calculated from the microscopic Hamiltonian. We can calculate the friction matrix and fluctuating force correlations based on this, as long as the bath and the system-bath coupling are linear. Even in the classical limit, the GLE is an ideal method to perform MD simulation, due to its stronger theoretical foundation compared to other approaches. For example, it fulfills the fluctuation-dissipation relation and ensures that the system can reach the canonical distribution in the long time limit[16]. Recently, algorithms aiming at application to realistic materials have been developed to efficiently treat the memory effect in the friction kernel and the colored noise spectrum[34, 35]. This opens the possibility of its application to realistic materials.

5. Conclusions

In this review, based on the influence functional approach, the classical Langevin equation is extended to include the quantum statistics and nonequilibrium features of the reservoir degrees of freedom. We have considered both phonon and electron reservoirs. These extensions result in a semi-classical generalized Langevin equation (SGLE), which can be used to study different problems that are difficult to handle using classical MD. The nuclear quantum effect in materials can be partly included through coupling to the quantum phonon baths. Phonon thermal transport can be studied by coupling the system to several phonon reservoirs with different temperatures. Atomic vibration, translation and rotation of adsorbates on metal surfaces are damped through the electron-hole pair excitation in the metal electrons. This is taken into account as the electronic friction in the SGLE. For nano-scale conductors in the presence of a current flow in the electronic reservoir, several interesting effects are predicted from the SGLE. Apart from the electronic and phononic reservoirs, a quantum thermal bath representing black body radiation has recently been used to study the radiative heat transfer from a black body to nearby dielectric nanoparticles[168]. This is possible since eigenmodes of electromagnetic waves and phonons are both represented by a set of harmonic oscillators. These results greatly extend the range of applications of the MD methods.

We also discussed the technical problems and available solutions in order to use the method to study realistic systems. The non-Markovian friction kernel can be transformed to a Markovian one by introducing auxiliary degrees of freedom. The colored noise can be generated on the fly during the MD simulation. The implementation of the quantum phonon bath in available molecular dynamics codes will further accelerate its application to the problems mentioned above. Several groups are working on this now, and it is believed that, these developments will enrich and widen the applications of MD.

Acknowledgements

The authors would like to thank Jian-Sheng Wang, Baowen Li, Tchavdar Todorov, Daniel Dundas, Nuo Yang, Tue Gunst, Rasmus B. Christensen, Nick R. Papior for discussions and collaborations on this subject. Financial support from the National Natural Science Foundation of China (grant number: 61371015), and the Villum Foundation (to MB, VKR00013340), is gratefully acknowledged.

References

References

- [1] I. R. Senitzky, Dissipation in Quantum Mechanics. The Harmonic Oscillator, *Phys. Rev. Lett.* 119 (2) (1960) 670–679.
- [2] I. R. Senitzky, Dissipation in Quantum Mechanics. The Harmonic Oscillator. II, *Phys. Rev. Lett.* 124 (3) (1961) 642–648.
- [3] M. Lax, Formal Theory of Quantum Fluctuations from a Driven State, *Phys. Rev. Lett.* 129 (5) (1963) 2342–2348.
- [4] H. Mori, Transport, Collective Motion, and Brownian Motion, *Prog. Theor. Phys.* 33 (3) (1965) 423–455.
- [5] S. Nordholm, R. Zwanzig, A systematic derivation of exact generalized Brownian motion theory, *J. Stat. Phys.* 13 (4) (1975) 347–371.
- [6] G.-L. Ingold, Path Integrals and Their Application to Dissipative Quantum Systems, in: *Coherent Evolution in Noisy Environments*, Lecture Notes in Physics, Springer, Berlin, Heidelberg, 2002, pp. 1–53.
- [7] H. Grabert, U. Weiss, P. Talkner, Quantum theory of the damped harmonic oscillator, *Z. Phys. B* 55 (1) (1984) 87–94.
- [8] P. Hänggi, G.-L. Ingold, Fundamental aspects of quantum Brownian motion, *Chaos* 15 (2) (2005) 026105.
- [9] C. Gardiner, P. Zoller, *Quantum Noise*, 3rd Edition, Springer-Verlag Berlin Heidelberg, 2004.
- [10] S. A. Adelman, J. D. Doll, Generalized Langevin equation approach for atom/solid surface scattering: Collinear atom/harmonic chain model, *J. Chem. Phys.* 61 (10) (1974) 4242–4245.
- [11] S. A. Adelman, J. D. Doll, Generalized Langevin equation approach for atom/solid surface scattering: General formulation for classical scattering off harmonic solids, *J. Chem. Phys.* 64 (6) (1976) 2375–2388.
- [12] A. Dhar, Heat Conduction in the Disordered Harmonic Chain Revisited, *Phys. Rev. Lett.* 86 (26) (2001) 5882–5885.
- [13] D. Segal, A. Nitzan, P. Hänggi, Thermal conductance through molecular wires, *J. Chem. Phys.* 119 (13) (2003) 6840–6855.
- [14] J.-S. Wang, Quantum Thermal Transport from Classical Molecular Dynamics, *Phys. Rev. Lett.* 99 (16) (2007) 160601.
- [15] L. Kantorovich, Generalized Langevin equation for solids. I. Rigorous derivation and main properties, *Phys. Rev. B* 78 (9) (2008) 094304.
- [16] L. Kantorovich, N. Rompotis, Generalized Langevin equation for solids. II. Stochastic boundary conditions for nonequilibrium molecular dynamics simulations, *Phys. Rev. B* 78 (9) (2008) 094305.
- [17] M. Ceriotti, G. Bussi, M. Parrinello, Nuclear Quantum Effects in Solids Using a Colored-Noise Thermostat, *Phys. Rev. Lett.* 103 (3) (2009) 030603.
- [18] H. Dammak, Y. Chalopin, M. Laroche, M. Hayoun, J.-J. Greffet, Quantum Thermal Bath for Molecular Dynamics Simulation, *Phys. Rev. Lett.* 103 (19) (2009) 190601.
- [19] H. Dammak, E. Antoshchenkova, M. Hayoun, F. Finocchi, Isotope effects in lithium hydride and lithium deuteride crystals by molecular dynamics simulations, *J. Phys. Condens. Matter* 24 (43) (2012) 435402.
- [20] M. Ceriotti, G. Bussi, M. Parrinello, Colored-Noise Thermostats la Carte, *J. Chem. Theory Comput.* 6 (4) (2010) 1170–1180.
- [21] F. Brieuc, Y. Bronstein, H. Dammak, P. Depondt, F. Finocchi, M. Hayoun, Zero-Point Energy Leakage in Quantum Thermal Bath Molecular Dynamics Simulations, *J. Chem. Theory Comput.* 12 (12) (2016) 5688–5697.
- [22] F. Brieuc, H. Dammak, M. Hayoun, Quantum Thermal Bath for Path Integral Molecular Dynamics Simulation, *J. Chem. Theory Comput.* 12 (3) (2016) 1351–1359.
- [23] S. Ganeshan, R. Ramírez, M. V. Fernández-Serra, Simulation of quantum zero-point effects in water using a frequency-dependent thermostat, *Phys. Rev. B* 87 (13) (2013) 134207.
- [24] Y. Bronstein, P. Depondt, L. E. Bove, R. Gaal, A. M. Saitta, F. Finocchi, Quantum versus classical protons in pure and salty ice under pressure, *Phys. Rev. B* 93 (2) (2016) 024104.
- [25] Y. Bronstein, P. Depondt, F. Finocchi, A. M. Saitta, Quantum-driven phase transition in ice described via an efficient Langevin approach, *Phys. Rev. B* 89 (21) (2014) 214101.
- [26] J. Guo, X.-Z. Li, J. Peng, E.-G. Wang, Y. Jiang, Atomic-scale investigation of nuclear quantum effects of surface water: Experiments and theory, *Prog. Surf. Sci.* 92 (4) (2017) 203–239.
- [27] A. Dhar, B. Sriram Shastry, Quantum transport using the Ford-Kac-Mazur formalism, *Phys. Rev. B* 67 (19) (2003) 195405.
- [28] L. W. Lee, A. Dhar, Heat Conduction in a Two-Dimensional Harmonic Crystal with Disorder, *Phys. Rev. Lett.* 95 (9) (2005) 094302.
- [29] A. Dhar, D. Roy, Heat Transport in Harmonic Lattices, *J. Stat. Phys.* 125 (4) (2006) 801–820.
- [30] J.-S. Wang, J. Wang, J. T. Lü, Quantum thermal transport in nanostructures, *Eur. Phys. J. B* 62 (4) (2008) 381–404.
- [31] D. Roy, Crossover from ballistic to diffusive thermal transport in quantum Langevin dynamics study of a harmonic chain connected to self-consistent reservoirs, *Phys. Rev. E* 77 (6) (2008) 062102.
- [32] J. T. Lü, J.-S. Wang, Coupled electronphonon transport from molecular dynamics with quantum baths, *J. Phys. Condens. Matter* 21 (2) (2009) 025503.
- [33] J.-S. Wang, X. Ni, J.-W. Jiang, Molecular dynamics with quantum heat baths: Application to nanoribbons and nanotubes, *Phys. Rev. B* 80 (22) (2009) 224302.
- [34] L. Stella, C. D. Lorenz, L. Kantorovich, Generalized Langevin equation: An efficient approach to nonequilibrium molecular dynamics of open systems, *Phys. Rev. B* 89 (13) (2014) 134303.

- [35] H. Ness, L. Stella, C. D. Lorenz, L. Kantorovich, Applications of the generalized Langevin equation: Towards a realistic description of the baths, *Phys. Rev. B* 91 (1) (2015) 014301.
- [36] N. Li, J. Ren, L. Wang, G. Zhang, P. Hänggi, B. Li, Colloquium, *Rev. Mod. Phys.* 84 (3) (2012) 1045–1066.
- [37] Y. A. Kosevich, A. V. Savin, A. Cantarero, Effects of quantum statistics of phonons on the thermal conductivity of silicon and germanium nanoribbons, *Nanoscale Res. Lett.* 8 (2013) 7.
- [38] P. Nieto, E. Pijper, D. Barredo, G. Laurent, R. A. Olsen, E.-J. Baerends, G.-J. Kroes, D. Farías, Reactive and Nonreactive Scattering of H₂ from a Metal Surface Is Electronically Adiabatic, *Science* 312 (5770) (2006) 86–89.
- [39] J. I. Juaristi, M. Alducin, R. D. Muiño, H. F. Busnengo, A. Salin, Role of electron-hole pair excitations in the dissociative adsorption of diatomic molecules on metal surfaces, *Phys. Rev. Lett.* 100 (11) (2008) 116102.
- [40] B. Jiang, M. Alducin, H. Guo, Electron-Hole Pair Effects in Polyatomic Dissociative Chemisorption: Water on Ni(111), *J. Phys. Chem. Lett.* 7 (2) (2016) 327–331.
- [41] D. Novko, M. Blanco-Rey, J. I. Juaristi, M. Alducin, Ab initio molecular dynamics with simultaneous electron and phonon excitations: Application to the relaxation of hot atoms and molecules on metal surfaces, *Phys. Rev. B* 92 (20) (2015) 201411.
- [42] G. Fuchsel, M. del Cueto, C. Díaz, G.-J. Kroes, Enigmatic HCl + Au(111) Reaction: A Puzzle for Theory and Experiment, *J. Phys. Chem. C* 120 (45) (2016) 25760–25779.
- [43] M. Grote Meyer, E. Pehlke, Electronic Energy Dissipation During Scattering of Vibrationally Excited Molecules at Metal Surfaces: Ab initio Simulations for HCl/Al(111), *Phys. Rev. Lett.* 112 (4) (2014) 043201.
- [44] H. Xin, J. LaRue, H. Öberg, M. Beye, M. Dell’Angela, J. J. Turner, J. Gladh, M. L. Ng, J. A. Sellberg, S. Kaya, G. Mercurio, F. Hieke, D. Nordlund, W. F. Schlotter, G. L. Dakovski, M. P. Miniti, A. Föhlisch, M. Wolf, W. Wurth, H. Ogasawara, J. K. Nørskov, H. Öström, L. G. M. Pettersson, A. Nilsson, F. Abild-Pedersen, Strong Influence of Coadsorbate Interaction on CO Desorption Dynamics on Ru(0001) Probed by Ultrafast X-Ray Spectroscopy and Ab Initio Simulations, *Phys. Rev. Lett.* 114 (15) (2015) 156101.
- [45] G. Fuchsel, T. Klamroth, S. Monturet, P. Saalfrank, Dissipative dynamics within the electronic friction approach: the femtosecond laser desorption of H₂/D₂ from Ru(0001), *Phys. Chem. Chem. Phys.* 13 (19) (2011) 8659–8670.
- [46] O. Bünermann, H. Jiang, Y. Dorenkamp, A. Kandratsenka, S. M. Janke, D. J. Auerbach, A. M. Wodtke, Electron-hole pair excitation determines the mechanism of hydrogen atom adsorption, *Science* 350 (6266) (2015) 1346–1349.
- [47] M. Blanco-Rey, J. I. Juaristi, R. Díez Muiño, H. F. Busnengo, G. J. Kroes, M. Alducin, Electronic Friction Dominates Hydrogen Hot-Atom Relaxation on Pd(100), *Phys. Rev. Lett.* 112 (10) (2014) 103203.
- [48] B. C. Krüger, N. Bartels, C. Bartels, A. Kandratsenka, J. C. Tully, A. M. Wodtke, T. Schäfer, NO Vibrational Energy Transfer on a Metal Surface: Still a Challenge to First-Principles Theory, *J. Phys. Chem. C* 119 (6) (2015) 3268–3272.
- [49] S. P. Rittmeyer, J. Meyer, J. I. Juaristi, K. Reuter, Electronic Friction-Based Vibrational Lifetimes of Molecular Adsorbates: Beyond the Independent-Atom Approximation, *Phys. Rev. Lett.* 115 (4) (2015) 046102.
- [50] M. Askerka, R. J. Maurer, V. S. Batista, J. C. Tully, Role of Tensorial Electronic Friction in Energy Transfer at Metal Surfaces, *Phys. Rev. Lett.* 116 (21) (2016) 217601.
- [51] R. J. Maurer, B. Jiang, H. Guo, J. C. Tully, Mode Specific Electronic Friction in Dissociative Chemisorption on Metal Surfaces: H-2 on Ag(111), *Phys. Rev. Lett.* 118 (25) (2017) 256001.
- [52] M. Galperin, A. Nitzan, Nuclear Dynamics at Molecule-Metal Interfaces: A Pseudoparticle Perspective, *J. Phys. Chem. Lett.* 6 (24) (2015) 4898–4903.
- [53] W. Dou, A. Nitzan, J. E. Subotnik, Frictional effects near a metal surface, *J. Chem. Phys.* 143 (5) (2015) 054103.
- [54] W. Dou, J. E. Subotnik, Universality of electronic friction: Equivalence of von Oppen’s nonequilibrium Green’s function approach and the Head-Gordon-Tully model at equilibrium, *Phys. Rev. B* 96 (10) (2017) 104305.
- [55] W. Dou, J. E. Subotnik, Electronic friction near metal surfaces: A case where molecule-metal couplings depend on nuclear coordinates, *J. Chem. Phys.* 146 (9) (2017) 092304.
- [56] W. Dou, G. Miao, J. E. Subotnik, Born-Oppenheimer Dynamics, Electronic Friction, and the Inclusion of Electron-Electron Interactions, *Phys. Rev. Lett.* 119 (4) (2017) 046001.
- [57] G. W. Ford, M. Kac, P. Mazur, Statistical Mechanics of Assemblies of Coupled Oscillators, *J. Math. Phys.* 6 (4) (1965) 504–515.
- [58] R. P. Feynman, F. L. Vernon, The theory of a general quantum system interacting with a linear dissipative system, *Ann. Phys. (N.Y.)* 24 (1963) 118–173.
- [59] G. M. G. McCaul, C. D. Lorenz, L. Kantorovich, Partition-free approach to open quantum systems in harmonic environments: An exact stochastic Liouville equation, *Phys. Rev. B* 95 (12) (2017) 125124.
- [60] L. Kantorovich, H. Ness, L. Stella, C. D. Lorenz, *c*-number quantum generalized langevin equation for an open system, *Phys. Rev. B* 94 (18) (2016) 184305.
- [61] A. O. Caldeira, A. J. Leggett, Influence of Dissipation on Quantum Tunneling in Macroscopic Systems, *Phys. Rev. Lett.* 46 (4) (1981) 211–214.
- [62] A. O. Caldeira, A. J. Leggett, Path integral approach to quantum Brownian motion, *Physica A* 121 (3) (1983) 587–616.
- [63] A. Schmid, On a quasiclassical Langevin equation, *J. Low Temp. Phys.* 49 (5-6) (1982) 609–626.
- [64] O. V. Prezhdo, Y. V. Pereverzev, Quantized Hamilton dynamics, *J. Chem. Phys.* 113 (16) (2000) 6557–6565.
- [65] O. V. Prezhdo, Y. V. Pereverzev, Quantized Hamilton dynamics for a general potential, *J. Chem. Phys.* 116 (11) (2002) 4450–4461.
- [66] O. V. Prezhdo, C. Brooksby, Non-adiabatic molecular dynamics with quantum solvent effects, *J. Mol. Struct.-Theochem* 630 (2003) 45–58.
- [67] O. V. Prezhdo, Quantized hamilton dynamics, *Theor. Chem. Acc.* 116 (1-3) (2006) 206–218.
- [68] M. Ceriotti, G. Bussi, M. Parrinello, Langevin Equation with Colored Noise for Constant-Temperature Molecular Dynamics Simulations, *Phys. Rev. Lett.* 102 (2) (2009) 020601.
- [69] M. Ceriotti, D. E. Manolopoulos, Efficient First-Principles Calculation of the Quantum Kinetic Energy and Momentum Distribution of Nuclei, *Phys. Rev. Lett.* 109 (10) (2012) 100604.
- [70] M. Ceriotti, W. Fang, P. G. Kusalik, R. H. McKenzie, A. Michaelides, M. A. Morales, T. E. Markland, Nuclear Quantum Effects in Water and Aqueous Systems: Experiment, Theory, and Current Challenges, *Chem. Rev.* 116 (13) (2016) 7529–7550.

- [71] F. Guinea, Friction and Particle-Hole Pairs, *Phys. Rev. Lett.* 53 (13) (1984) 1268–1271.
- [72] L.-D. Chang, S. Chakravarty, Dissipative dynamics of a two-state system coupled to a heat bath, *Phys. Rev. B* 31 (1) (1985) 154–164.
- [73] P. Hedegård, A. O. Caldeira, Quantum Dynamics of a Particle in a Fermionic Environment, *Phys. Scr.* 35 (5) (1987) 609.
- [74] P. Hedegård, Light quantum particles in a metallic environment, *Phys. Rev. B* 35 (2) (1987) 533–544.
- [75] M. Persson, B. Hellsing, Electronic Damping of Adsorbate Vibrations on Metal Surfaces, *Phys. Rev. Lett.* 49 (9) (1982) 662–665.
- [76] B. Hellsing, M. Persson, Electronic Damping of Atomic and Molecular Vibrations at Metal Surfaces, *Phys. Scr.* 29 (4) (1984) 360.
- [77] P. Avouris, B. N. J. Persson, Excited states at metal surfaces and their non-radiative relaxation, *J. Phys. Chem.* 88 (5) (1984) 837–848.
- [78] B. N. J. Persson, Surface resistivity and vibrational damping in adsorbed layers, *Phys. Rev. B* 44 (7) (1991) 3277–3296.
- [79] M. Head-Gordon, J. C. Tully, Vibrational relaxation on metal surfaces: Molecular-orbital theory and application to CO/Cu(100), *J. Chem. Phys.* 96 (5) (1992) 3939–3949.
- [80] M. Head-Gordon, J. C. Tully, Molecular-orbital calculations of the lifetimes of the vibrational modes of CO on Cu(100), *Phys. Rev. B* 46 (3) (1992) 1853–1856.
- [81] M. Head-Gordon, J. C. Tully, Molecular dynamics with electronic frictions, *J. Chem. Phys.* 103 (23) (1995) 10137–10145.
- [82] M. Brandbyge, P. Hedegård, Theory of the Egler switch, *Phys. Rev. Lett.* 72 (18) (1994) 2919–2922.
- [83] M. Brandbyge, P. Hedegård, T. F. Heinz, J. A. Misewich, D. M. Newns, Electronically driven adsorbate excitation mechanism in femtosecond-pulse laser desorption, *Phys. Rev. B* 52 (8) (1995) 6042–6056.
- [84] D. Mozyrsky, I. Martin, M. B. Hastings, Quantum-Limited Sensitivity of Single-Electron-Transistor-Based Displacement Detectors, *Phys. Rev. Lett.* 92 (1) (2004) 018303.
- [85] D. Mozyrsky, M. B. Hastings, I. Martin, Intermittent polaron dynamics: Born-Oppenheimer approximation out of equilibrium, *Phys. Rev. B* 73 (3) (2006) 035104.
- [86] J. Daligault, D. Mozyrsky, Non-Adiabatic Quantum Molecular Dynamics with Detailed Balance, arXiv:1708.06679.
- [87] J.-T. Lü, M. Brandbyge, P. Hedegård, Blowing the Fuse: Berry’s Phase and Runaway Vibrations in Molecular Conductors, *Nano Lett.* 10 (5) (2010) 1657–1663.
- [88] J.-T. Lü, P. Hedegård, M. Brandbyge, Laserlike Vibrational Instability in Rectifying Molecular Conductors, *Phys. Rev. Lett.* 107 (4) (2011) 046801.
- [89] J.-T. Lü, T. Gunst, P. Hedegård, M. Brandbyge, Current-induced dynamics in carbon atomic contacts, *Beilstein J. Nanotechnol.* 2 (2011) 814–823.
- [90] J.-T. Lü, M. Brandbyge, P. Hedegård, T. N. Todorov, D. Dundas, Current-induced atomic dynamics, instabilities, and Raman signals: Quasiclassical Langevin equation approach, *Phys. Rev. B* 85 (24) (2012) 245444.
- [91] T. Gunst, J.-T. Lü, P. Hedegård, M. Brandbyge, Phonon excitation and instabilities in biased graphene nanoconstrictions, *Phys. Rev. B* 88 (16) (2013) 161401.
- [92] J.-T. Lü, R. B. Christensen, J.-S. Wang, P. Hedegård, M. Brandbyge, Current-Induced Forces and Hot Spots in Biased Nanojunctions, *Phys. Rev. Lett.* 114 (9) (2015) 096801.
- [93] N. Bode, S. V. Kusminskiy, R. Egger, F. von Oppen, Scattering Theory of Current-Induced Forces in Mesoscopic Systems, *Phys. Rev. Lett.* 107 (3) (2011) 036804.
- [94] N. Bode, S. V. Kusminskiy, R. Egger, F. v. Oppen, Current-induced forces in mesoscopic systems: A scattering-matrix approach, *Beilstein J. Nanotechnol.* 3 (1) (2012) 144–162.
- [95] R. Hussein, A. Metelmann, P. Zedler, T. Brandes, Semiclassical dynamics of nanoelectromechanical systems, *Phys. Rev. B* 82 (16) (2010) 165406.
- [96] A. Metelmann, T. Brandes, Adiabaticity in semiclassical nanoelectromechanical systems, *Phys. Rev. B* 84 (15) (2011) 155455.
- [97] A. Metelmann, T. Brandes, Transport through single-level systems: Spin dynamics in the nonadiabatic regime, *Phys. Rev. B* 86 (24) (2012) 245317.
- [98] C. López-Monís, C. Emary, G. Kiesslich, G. Platero, T. Brandes, Limit cycles and chaos in the current through a quantum dot, *Phys. Rev. B* 85 (4) (2012) 045301.
- [99] K. Mosshammer, T. Brandes, Semiclassical spin-spin dynamics and feedback control in transport through a quantum dot, *Phys. Rev. B* 90 (13) (2014) 134305.
- [100] N. Hashitsume, M. Mori, T. Takahashi, A Derivation of Generalized Semi-Classical Langevin Equations Based on the Feynman Path-Integral Approach, *J. Phys. Soc. Jpn.* 55 (6) (1986) 1887–1893.
- [101] C. W. Gardiner, Quantum noise and quantum Langevin equations, *IBM J. Res. Dev.* 32 (1) (1988) 127–136.
- [102] H. Kleinert, S. V. Shabanov, Quantum Langevin equation from forward-backward path integral, *Phys. Lett. A* 200 (3) (1995) 224–232.
- [103] A. P. Horsfield, D. R. Bowler, A. J. Fisher, T. N. Todorov, M. J. Montgomery, Power dissipation in nanoscale conductors: classical, semi-classical and quantum dynamics, *J. Phys. Condens. Matter* 16 (21) (2004) 3609.
- [104] A. Abedi, F. Agostini, E. K. U. Gross, Mixed quantum-classical dynamics from the exact decomposition of electron-nuclear motion, *Europhys. Lett.* 106 (3) (2014) 33001.
- [105] A. Abedi, N. T. Maitra, E. K. U. Gross, Exact Factorization of the Time-Dependent Electron-Nuclear Wave Function, *Phys. Rev. Lett.* 105 (12) (2010) 123002.
- [106] M. Thomas, T. Karzig, S. V. Kusminskiy, G. Zaránd, F. von Oppen, Scattering theory of adiabatic reaction forces due to out-of-equilibrium quantum environments, *Phys. Rev. B* 86 (19) (2012) 195419.
- [107] Y. Wang, L. Kantorovich, Nonequilibrium statistical mechanics of classical nuclei interacting with the quantum electron gas, *Phys. Rev. B* 76 (14) (2007) 144304.
- [108] H. Lei, N. A. Baker, X. Li, Data-driven parameterization of the generalized Langevin equation, *Proc. Natl. Acad. Sci.* 113 (50) (2016) 14183–14188.
- [109] H. Ness, A. Genina, L. Stella, C. D. Lorenz, L. Kantorovich, Nonequilibrium processes from generalized Langevin equations: Realistic nanoscale systems connected to two thermal baths, *Phys. Rev. B* 93 (17) (2016) 174303.
- [110] A. A. Dzhioev, D. S. Kosov, Kramers problem for nonequilibrium current-induced chemical reactions, *J. Chem. Phys.* 135 (7) (2011)

- 074701.
- [111] A. A. Dzhioev, D. S. Kosov, F. von Oppen, Out-of-equilibrium catalysis of chemical reactions by electronic tunnel currents, *J. Chem. Phys.* 138 (13) (2013) 134103.
 - [112] J.-T. Lü, H. Zhou, J.-W. Jiang, J.-S. Wang, Effects of electron-phonon interaction on thermal and electrical transport through molecular nano-conductors, *AIP Adv.* 5 (5) (2015) 053204.
 - [113] R. Bustos-Marín, G. Refael, F. von Oppen, Adiabatic Quantum Motors, *Phys. Rev. Lett.* 111 (6) (2013) 060802.
 - [114] V. Krishna, J. C. Tully, Vibrational lifetimes of molecular adsorbates on metal surfaces, *J. Chem. Phys.* 125 (5) (2006) 054706.
 - [115] H.-C. Chang, G. E. Ewing, Infrared fluorescence from a monolayer of CO on NaCl(100), *Phys. Rev. Lett.* 65 (17) (1990) 2125–2128.
 - [116] J. D. White, J. Chen, D. Matsiev, D. J. Auerbach, A. M. Wodtke, Conversion of large-amplitude vibration to electron excitation at a metal surface, *Nature* 433 (7025) (2005) 503–505.
 - [117] X. Yang, E. H. Kim, A. M. Wodtke, Vibrational energy transfer of very highly vibrationally excited NO, *J. Chem. Phys.* 96 (7) (1992) 5111–5122.
 - [118] H. Nienhaus, H. S. Bergh, B. Gergen, A. Majumdar, W. H. Weinberg, E. W. McFarland, Electron-Hole Pair Creation at Ag and Cu Surfaces by Adsorption of Atomic Hydrogen and Deuterium, *Phys. Rev. Lett.* 82 (2) (1999) 446–449.
 - [119] B. Gergen, H. Nienhaus, W. H. Weinberg, E. W. McFarland, Chemically Induced Electronic Excitations at Metal Surfaces, *Science* 294 (5551) (2001) 2521–2523.
 - [120] J. R. Trail, M. C. Graham, D. M. Bird, M. Persson, S. Holloway, Energy Loss of Atoms at Metal Surfaces due to Electron-Hole Pair Excitations: First-Principles Theory of “Chemicurrents”, *Phys. Rev. Lett.* 88 (16) (2002) 166802.
 - [121] L. Simine, D. Segal, Vibrational cooling, heating, and instability in molecular conducting junctions: full counting statistics analysis, *Phys. Chem. Chem. Phys.* 14 (40) (2012) 13820–13834.
 - [122] R. Landauer, J. W. F. Woo, Driving force in electromigration, *Phys. Rev. B* 10 (4) (1974) 1266–1271.
 - [123] L. J. Sham, Microscopic theory of the driving force in electromigration, *Phys. Rev. B* 12 (8) (1975) 3142–3149.
 - [124] R. S. Sorbello, B. Dasgupta, Local fields in electron transport: Application to electromigration, *Phys. Rev. B* 16 (1977) 5193–5205.
 - [125] M. Di Ventura, Y.-C. Chen, T. N. Todorov, Are Current-Induced Forces Conservative?, *Phys. Rev. Lett.* 92 (17) (2004) 176803.
 - [126] D. Dundas, E. J. McEniry, T. N. Todorov, Current-driven atomic waterwheels, *Nature Nanotech.* 4 (2) (2009) 99–102.
 - [127] T. N. Todorov, D. Dundas, E. J. McEniry, Nonconservative generalized current-induced forces, *Phys. Rev. B* 81 (7) (2010) 075416.
 - [128] T. N. Todorov, D. Dundas, A. T. Paxton, A. P. Horsfield, Nonconservative current-induced forces: A physical interpretation, *Beilstein J. Nanotechnol.* 2 (1) (2011) 727–733.
 - [129] E. J. McEniry, Y. Wang, D. Dundas, T. N. Todorov, L. Stella, R. P. Miranda, A. J. Fisher, A. P. Horsfield, C. P. Race, D. R. Mason, W. M. C. Foulkes, A. P. Sutton, Modelling non-adiabatic processes using correlated electron-ion dynamics, *Eur. Phys. J. B* 77 (3) (2010) 305–329.
 - [130] L. J. Fernández-Alcázar, R. A. Bustos-Marín, H. M. Pastawski, Decoherence in current induced forces: Application to adiabatic quantum motors, *Phys. Rev. B* 92 (7) (2015) 075406.
 - [131] L. J. Fernández-Alcázar, H. M. Pastawski, R. A. Bustos-Marín, Dynamics and decoherence in nonideal Thouless quantum motors, *Phys. Rev. B* 95 (15) (2017) 155410.
 - [132] H. L. Calvo, F. D. Ribetto, R. A. Bustos-Marín, Real-time diagrammatic approach to current-induced forces: Application to quantum-dot based nanomotors, *Phys. Rev. B* 96 (16) (2017) 165309.
 - [133] M. V. Berry, J. M. Robbins, Chaotic classical and half-classical adiabatic reactions: geometric magnetism and deterministic friction, *Proc. R. Soc. Lond. A* 442 (1916) (1993) 659–672.
 - [134] K. Lü, J.-D. Bao, Numerical simulation of generalized Langevin equation with arbitrary correlated noise, *Phys. Rev. E* 72 (6) (2005) 067701.
 - [135] J.-L. Barrat, D. Rodney, Portable Implementation of a Quantum Thermal Bath for Molecular Dynamics Simulations, *J. Stat. Phys.* 144 (3) (2011) 679–689.
 - [136] J. Schmidt, A. Meistrenko, H. van Hees, Z. Xu, C. Greiner, Simulation of stationary Gaussian noise with regard to the Langevin equation with memory effect, *Phys. Rev. E* 91 (3) (2015) 032125.
 - [137] M. Morin, N. J. Levinos, A. L. Harris, Vibrational energy transfer of CO/Cu(100): Nonadiabatic vibration/electron coupling, *J. Chem. Phys.* 96 (5) (1992) 3950–3956.
 - [138] M. Alducin, R. Dez Muio, J. I. Juaristi, Non-adiabatic effects in elementary reaction processes at metal surfaces, *Prog. Surf. Sci.* 92 (4) (2017) 317–340.
 - [139] C. T. Rettner, F. Fabre, J. Kimman, D. J. Auerbach, Observation of Direct Vibrational Excitation in Gas-Surface Collisions: NO on Ag(111), *Phys. Rev. Lett.* 55 (18) (1985) 1904–1907.
 - [140] C. T. Rettner, J. Kimman, F. Fabre, D. J. Auerbach, H. Morawitz, Direct vibrational excitation in gas-surface collisions of NO with Ag(111), *Surf. Sci.* 192 (1) (1987) 107–130.
 - [141] X. Yang, A. M. Wodtke, Controlling the quantum numbers in chemical reactions, *Int. Rev. Phys. Chem.* 12 (1) (1993) 123–147.
 - [142] T. Vazhappilly, T. Klamroth, P. Saalfrank, R. Hernandez, Femtosecond-Laser Desorption of H-2 (D-2) from Ru(0001): Quantum and Classical Approaches, *J. Phys. Chem. C* 113 (18) (2009) 7790–7801.
 - [143] G. Fuchselsel, J. C. Tremblay, T. Klamroth, P. Saalfrank, C. Frischkorn, Concept of a Single Temperature for Highly Nonequilibrium Laser-Induced Hydrogen Desorption from a Ruthenium Surface, *Phys. Rev. Lett.* 109 (9) (2012) 098303.
 - [144] R. Scholz, G. Floß, P. Saalfrank, G. Fuchselsel, I. Lončarić, J. I. Juaristi, Femtosecond-laser induced dynamics of CO on Ru(0001): Deep insights from a hot-electron friction model including surface motion, *Phys. Rev. B* 94 (16) (2016) 165447.
 - [145] X. Luo, B. Jiang, J. I. Juaristi, M. Alducin, H. Guo, Electron-hole pair effects in methane dissociative chemisorption on Ni(111), *J. Chem. Phys.* 145 (4) (2016) 044704.
 - [146] G.-J. Kroes, J. I. Juaristi, M. Alducin, Vibrational Excitation of H-2 Scattering from Cu(111): Effects of Surface Temperature and of Allowing Energy Exchange with the Surface, *J. Phys. Chem. C* 121 (25) (2017) 13617–13633.
 - [147] G. Fuchselsel, J. C. Tremblay, T. Klamroth, P. Saalfrank, C. Frischkorn, Concept of a Single Temperature for Highly Nonequilibrium Laser-Induced Hydrogen Desorption from a Ruthenium Surface, *Phys. Rev. Lett.* 109 (9) (2012) 098303.
 - [148] M. Tsutsui, T. Kawai, M. Taniguchi, Unsymmetrical hot electron heating in quasi-ballistic nanocontacts, *Sci. Rep.* 2 (2012) 217.

- [149] C. Schirm, M. Matt, F. Pauly, J. C. Cuevas, P. Nielaba, E. Scheer, A current-driven single-atom memory, *Nature Nanotech.* 8 (9) (2013) 645.
- [150] T. Gunst, Transport and dynamics of nanostructured graphene, Ph.D. thesis, Technical University of Denmark (2014).
- [151] R. B. Christensen, J.-T. Lü, P. Hedegård, M. Brandbyge, Current-induced runaway vibrations in dehydrogenated graphene nanoribbons, *Beilstein J. Nanotechnol.* 7 (2016) 68–74.
- [152] M. Brandbyge, K. Stokbro, J. Taylor, J.-L. Mozos, P. Ordejón, Origin of current-induced forces in an atomic gold wire: A first-principles study, *Phys. Rev. B* 67 (19) (2003) 193104.
- [153] C. Cazorla, J. Boronat, Simulation and understanding of atomic and molecular quantum crystals, *Rev. Mod. Phys.* 89 (3) (2017) 035003.
- [154] X.-Z. Li, B. Walker, A. Michaelides, Quantum nature of the hydrogen bond, *Proc. Natl. Acad. Sci.* 108 (16) (2011) 6369–6373.
- [155] A. H. Barrozo, M. de Koninck, Comment on “Quantum Thermal Bath for Molecular Dynamics Simulation”, *Phys. Rev. Lett.* 107 (19) (2011) 198901.
- [156] H. Dammak, M. Hayoun, Y. Chalopin, J.-J. Greffet, Dammak et al. Reply:, *Phys. Rev. Lett.* 107 (19) (2011) 198902.
- [157] F. Calvo, N.-T. Van-Oanh, P. Parneix, C. Falvo, Vibrational spectra of polyatomic molecules assisted by quantum thermal baths, *Phys. Chem. Chem. Phys.* 14 (30) (2012) 10503–10506.
- [158] F. Calvo, C. Falvo, P. Parneix, Atomistic Modeling of Vibrational Action Spectra in Polyatomic Molecules: Nuclear Quantum Effects, *J. Phys. Chem. A* 118 (29) (2014) 5427–5436.
- [159] T. Qi, E. J. Reed, Simulations of Shocked Methane Including Self-Consistent Semiclassical Quantum Nuclear Effects, *J. Phys. Chem. A* 116 (42) (2012) 10451–10459.
- [160] Y. Shen, E. J. Reed, Quantum Nuclear Effects in Stishovite Crystallization in Shock-Compressed Fused Silica, *J. Phys. Chem. C* 120 (31) (2016) 17759–17766.
- [161] C. H. Woo, H. Wen, A. A. Semenov, S. L. Dudarev, P.-W. Ma, Quantum heat bath for spin-lattice dynamics, *Phys. Rev. B* 91 (10) (2015) 104306.
- [162] T. D. Swinburne, P.-W. Ma, S. L. Dudarev, Low temperature diffusivity of self-interstitial defects in tungsten, *New J. Phys.* 19 (7) (2017) 073024.
- [163] L. Bergqvist, A. Bergman, Realistic finite temperature simulations of magnetic systems using quantum statistics, arXiv:1708.00709.
- [164] M. Ceriotti, M. Parrinello, T. E. Markland, D. E. Manolopoulos, Efficient stochastic thermostating of path integral molecular dynamics, *J. Chem. Phys.* 133 (12) (2010) 124104.
- [165] O. N. Bedoya-Martínez, J.-L. Barrat, D. Rodney, Computation of the thermal conductivity using methods based on classical and quantum molecular dynamics, *Phys. Rev. B* 89 (1) (2014) 014303.
- [166] G. Czako, A. L. Kaledin, J. M. Bowman, A practical method to avoid zero-point leak in molecular dynamics calculations: Application to the water dimer, *J. Chem. Phys.* 132 (16) (2010) 164103.
- [167] K. Säskilähti, J. Oksanen, J. Tulkki, Thermal balance and quantum heat transport in nanostructures thermalized by local Langevin heat baths, *Phys. Rev. E* 88 (1) (2013) 012128.
- [168] Y. Chalopin, H. Dammak, M. Laroche, M. Hayoun, J.-J. Greffet, Radiative heat transfer from a black body to dielectric nanoparticles, *Phys. Rev. B* 84 (22) (2011) 224301.